Vol. 484: 155–171, 2013
doi: 10.3354/meps10305

MARINE ECOLOGY PROGRESS SERIES
Mar Ecol Prog Ser

Published June 12

Why the size structure of marine communities can require decades to recover from fishing

Tak Fung[1,*], Keith D. Farnsworth[1], Samuel Shephard[2], David G. Reid[3], Axel G. Rossberg[1,4]

[1]Queen's University Belfast, School of Biological Sciences, Belfast BT9 7BL, UK
[2]Marine and Freshwater Research Centre, Department of Life Sciences, Galway-Mayo Institute of Technology, Galway, Ireland
[3]Marine Institute, Fisheries Science Services, Rinville, Oranmore, Galway, Ireland
[4]Centre for Environment, Fisheries and Aquaculture Science (Cefas), Lowestoft, Suffolk NR33 0HT, UK

ABSTRACT: A dynamic food-web model of more than 1000 species was used to quantify the recovery trajectory of marine community size-structure under different hypothetical fishing regimes, using the Northeast Atlantic as an example. Size-structure was summarised by 4 indicators: the Large Fish Indicator (LFI), the Large Species Indicator (LSI), the biomass-weighted mean maximum length of fish species ($\overline{L}_{max}$) and the biomass-weighted mean maturation length of fish species ($\overline{L}_{mat}$). Time-series of these indicators recorded recovery following release from fishing with various size-selectivities, intensities and durations. In model simulations, fishing-induced trophic cascades were observed to distort fish community size-structure, but these did not have a large influence on recovery level or duration as measured by the 4 indicators. However, simulations showed that local extinctions of large fish species increased in number with both fishing intensity and duration, and could strongly limit the recovery level. Recovery of fish community size-structure to near equilibrium frequently took multiple decades in simulations; these long transient periods suggest that management interventions for size-structure recovery may require much longer than previously thought. Our results demonstrate the need for community-level modelling to set realistic targets for management of community size-structure.

KEY WORDS: Ecosystem approach to fisheries management · Food-web · Resilience · Dynamic model · Fisheries indicators · Extinction · Species richness

INTRODUCTION

Fishing probably exerts the greatest anthropogenic effect on coastal marine communities worldwide (Jackson et al. 2001, Tremblay-Boyer et al. 2011) and is second only to climate change when whole oceans are considered (Halpern et al. 2008). Myers & Worm (2003) estimated that, worldwide, industrialised fisheries have reduced the biomass of large predatory fish to just 10% of pre-industrial levels, while Worm et al. (2009) estimated that 63% of assessed fish stocks have a biomass below the level corresponding to maximum sustainable yield (MSY). The recovery of these fish populations is of direct interest to fisheries management, and since the fish are part of wider ecological systems, it is also important to general marine conservation.

In 2002, the UN World Summit on Sustainable Development (WSSD) committed signatory governments to restore world fish stocks to levels producing MSY by 2015 (Johannesburg Plan of Implementation 2002). However, achieving this target has been hindered by over-reliance on single-species fisheries management approaches (Pauly et al. 2002) that fail

*Email: tfung01@qub.ac.uk

to account for strong ecological interactions among exploited and non-target species (Frank et al. 2005, Scheffer et al. 2005). Conserving whole marine communities is now understood to be the necessary foundation for recovery of important individual species, this concept being expressed in the 'Ecosystem Approach to Fisheries Management' (EAFM; Pikitch et al. 2004). In 2003, the Food and Agriculture Organization of the United Nations (FAO) defined EAFM and provided guidelines for the translation of EAFM policy goals into actions (FAO 2003), thus facilitating its uptake. Currently, EAFM has been adopted by a number of countries, including Canada (Oceans Act; Department of Justice Canada 2005) and the USA (Magnuson-Stevens Fishery Conservation and Management Act; NOAA 2007), as well as the EU (Marine Strategy Framework Directive; EU 2008). However, there is concern that community recovery may take much longer than recovery of a single species (Murawski 2010), and this is supported by empirical evidence. From a quantitative review of marine reserve performances, Babcock et al. (2010) concluded that restoration of individual species can be delayed by indirect, cascading trophic interactions, which take place on longer timescales than the direct response of target species. In addition, Frank et al. (2011) describe trophic cascades as greatly delaying recovery from heavy fishing in the eastern Scotian Shelf system; cascade effects were seen to propagate throughout the food-web more than 15 yr after strict fishing restrictions were initiated. Since mixed (multispecies) fisheries are common, a community-level understanding of recovery dynamics is essential to predict conservation outcomes. Unfortunately, the direct modelling of a whole food-web is rarely supported by available data, and the same problem limits direct assessment of community composition for EAFM targets. However, to a first approximation, body size is a good surrogate for trophic level (Jennings et al. 2001). This has motivated the use of (1) statistics summarising community size-structure as indicators of community 'quality' (reviewed by Shin et al. 2005) and (2) size-structured models of community dynamics (e.g. Benoît & Rochet 2004, Shin & Cury 2004, Andersen & Beyer 2006, Blanchard et al. 2009, 2011, Hartvig et al. 2011, Houle et al. 2012, Rossberg 2012, Rochet & Benoît 2012), which have parsimonious data requirements for parameterisation, to predict the response of community size-structure indicators to fisheries management.

Conservation of community size-structure is a component of the FAO Code of Conduct for Responsible Fisheries (FAO 1995) and has recently been adopted into EAFM by the EU, where it appears as part of the Marine Strategy Framework Directive (Descriptor 4 — Food webs; EU 2008). Accordingly, in this paper we focus on the recovery of community size-structure, by investigating both the transient and long-term (equilibrium) dynamics of a model community following simulated reductions in fishing pressure. A realistic model must represent size-structure in marine communities spanning 8 or more orders of magnitude in body size (Boudreau & Dickie 1992) and also represent the dynamics of over 100 fish species populations, as typically found in marine communities (see, e.g. lists of fish species produced using the 'Information by Ecosystem' tool and 'All fishes' option at www.fishbase.org [Froese & Pauly 2010]); models with fewer populations may fail to capture whole community dynamics (McCann 2000). We find these desirable properties in the Population-Dynamical Matching Model (PDMM) of Rossberg et al. (2008), which is a size-structured multispecies model of a dynamic food-web. As we demonstrate in this study, the PDMM is capable of generating dynamically stable model marine communities with a body size range spanning over 15 orders of magnitude, encompassing phytoplankton to large fish, and with a fish species richness of >100. This contrasts with other dynamic marine community or ecosystem models (e.g. Hall et al. 2006, Speirs et al. 2010, Hartvig et al. 2011), which typically describe fewer than 30 coexisting fish species (Plagányi 2007) and hence may seriously under-represent the number of direct and indirect interactions. The PDMM achieves dynamic stability of species-rich communities using a stochastic assembly algorithm that does not require invoking insufficiently documented or speculative ecological mechanisms. Thus, the PDMM resolves a long-standing problem that was, in the context of marine community modelling, first described by Andersen & Ursin (1977, Sec 2.4): empirically parameterised models of speciose food-webs tend to be dynamically unstable unless sufficiently strong non-trophic intraspecific competition is introduced (e.g. Andersen & Ursin 1977, Loeuille & Loreau 2005, Andersen & Pedersen 2010, Hartvig et al. 2011). Production and hence stability of consumer species populations in the PDMM depend on trophic interactions — production is a function of resource abundances, in agreement with empirical studies (Anderson 2001, Jeschke et al. 2004, Moustahfid et al. 2010), rather than being independent of resource abundances (Hall et al. 2006, Speirs et al. 2010).

We use the PDMM to simulate a temperate shelf community in the Northeast Atlantic, a region that has a long and well-documented history of fisheries

and their community effects. The example community represents 189 distinct fish species populations set within a community of over a thousand species-distinct populations, including phytoplankton and zooplankton. We use the model to examine the transient and equilibrium response of a temperate shelf community under a suite of fisheries management scenarios, and thus to obtain predictions of the extent and rate of recovery in community size-structure under these scenarios. Community size-structure is summarised by a total of 4 indicators. Trends in these size-structure indicators are compared to trends in total fish biomass density, an indicator of system resource size (Rochet & Trenkel 2003, Cury et al. 2005). Together with the general properties of the model used, our results thus provide a general explanation for the transient and equilibrium behaviour of community size-structure under changing fisheries management. We highlight the general features of most importance to conservation-oriented fisheries management.

MATERIALS AND METHODS

A realistic dynamic model community is experimentally subjected to different fishing regimes and then allowed to recover under reduced fishing pressure. We measure the transient and equilibrium responses in this community using 4 size-structure indicators and 1 indicator of resource size, all of which can be used in fisheries management.

Indicators considered

A recent analysis of the sensitivity and specificity of size-structure indicators in fisheries management (Houle et al. 2012) has shown that the Large Fish Indicator (LFI) and its close relative the Large Species Indicator (LSI) are among the best-performing. In addition, both of these indicators can be computed directly from survey data. Therefore, the LFI and LSI are used in this study. The LFI measures the biomass of individual fish above a length threshold (large fish) as a proportion of total fish biomass (Greenstreet et al. 2011). LFI captures changes in relative species abundances and changes in intraspecific size-structures (Greenstreet et al. 2011, Shephard et al. 2011) and has been adopted by OSPAR to define an Ecological Quality Objective (EcoQO) for a fish community (Heslenfeld & Enserink 2008, Greenstreet et al. 2011). It has also been listed as a food-web indicator in the EU's Marine Strategy Framework Directive (EU 2008, EC 2010). The LSI is defined as the proportion of fish community biomass belonging to species with maximum length above a threshold that defines large species (Shin et al. 2010, Shephard et al. 2012), so it is specifically sensitive to changes in relative species abundances.

The size-structure of a fish community can also be characterised by length-based indicators, and we use 2 of these in our simulation study: the mean maximum length of fish species (Jennings et al. 1999, Shin et al. 2005), $\bar{L}_{max}$, and the mean maturation length of fish species (Jennings et al. 1999, Shin et al. 2005, Greenstreet & Rogers 2006), $\bar{L}_{mat}$. These 2 mean lengths are calculated using biomass rather than abundance as weights, because the former has been found to consistently give greater sensitivity and specificity to fishing for length-based indicators (Houle et al. 2012).

For fished marine ecosystems, changes in the distribution of total fish biomass, or total fish biomass density, among different size categories underlie the responses of all indicators of fish community size-structure. In addition, total fish biomass or total fish biomass density can be used as a proxy for total fish biomass productivity, and hence as an indicator of resource size for fisheries (Rochet & Trenkel 2003, Cury et al. 2005). Therefore, to complement the 4 size-structure indicators, total fish biomass density, B_{tot}, is considered in this study as well. Other types of indicators are available that incorporate other aspects of community structure and functioning, such as the trophic level of species and the evenness of distribution of biomass among species. These include the mean trophic level (Branch et al. 2010), Pielou's species evenness (Rochet et al. 2011) and Hill's N1 (Hall et al. 2006), which is the exponential of the Shannon-Wiener Index. However, these other types of indicators are not investigated in this study because the focus of the present study is on community size-structure.

Outline of model structure

The PDMM (Rossberg et al. 2008) describes community dynamics through a set of coupled non-linear ordinary differential equations, each representing the biomass dynamics of one species population. A full description of the model equations, including all the parameters and variables, are given in the Supplement at www.int-res.com/articles/suppl/m484p155_supp.pdf. Here, only the main features of the PDMM are described.

Associated with each species in the PDMM is a maturation body mass, determining its maximum growth rate and its consumption-independent loss rate (representing losses mainly through metabolism but also including mortality arising from processes other than consumption) from allometric scaling laws (Niklas & Enquist 2001, Brown et al. 2004, Savage et al. 2004). The consumption rate of a resource species i eaten by a consumer species j is defined by an extended Holling-Type II functional response, f_{ij}, based on van Leeuwen et al. (2007) (see the Supplement for details). This incorporates prey-switching by consumers, i.e. the tendency of consumers to concentrate foraging on the more abundant resources (May 1977). For a consumer and a resource species in the PDMM, trophic interaction strengths depend on their relative body masses and on sets of abstract traits that position a species as consumer (foraging traits) and as resource (vulnerability traits) in trophic niche space (Yoshida 2003, Rossberg et al. 2010). Size preference is parameterised by a preferred predator-prey body mass ratio (Jennings et al. 2002). Interaction strengths are large if a resource (species) is in the consumer's preferred size range and if the position in trophic niche space given by the resource's vulnerability traits is close to the position given by the foraging traits of the consumer. This trophic trait matching has been shown to lead to food-web topologies similar to those seen in natural terrestrial and aquatic communities (Rossberg et al. 2006, Rossberg et al. 2008). In a similar way, the match between abstract competition traits of 2 producer species determines the strength of competition between them for limiting resources, such as light and nutrients.

Model community assembly

Maturation body masses and vulnerability traits of all species, foraging traits of consumers, and competition traits of producers are determined through an iterative algorithm that mimics the assembly process of complex ecological communities (Rossberg et al. 2008; see also algorithms used in models by Post & Pimm 1983, Drake 1990, Law & Morton 1996, Caldarelli et al. 1998). Starting from a small community, new species that differ from resident species by small changes of their traits are added iteratively to the community, while species that go extinct in the extended community are removed in each iteration. This method leads to large, stable communities without the need for additional, stabilising density dependencies. Constructing ecological models using such a developmental approach (sensu Taylor 1989) creates phylogenetic constraints of the kind observed in natural food-webs (Cattin et al. 2004, Bersier & Kehrli 2008) whereby related species have similar sets of consumers and resources. Full details of the assembly algorithm are given in the Supplement.

Model parameterisation

The PDMM was parameterised for a temperate shelf community in the Northeast Atlantic, using empirical data from that region where possible and data from marine communities in other regions. An important outcome of the chosen parameterisation is that the predator-prey body mass ratio window for each consumer species population is wide (see Eq. S17a,b and Fig. S2 in the Supplement). This wide window is expected from a comprehensive analytic theory of the dynamics of size-structured marine communities (Rossberg 2012, Section IX.C), and reflects the widely differing food sources used by consumers at different ontogenetic stages of their growth. Details of the parameterisation methodology, which largely follow Rossberg et al. (2008), and the parameter values derived are given in the Supplement, including a more detailed justification of the use of wide predator-prey mass ratio windows.

Model validation

Only very simple, if any, marine communities have been studied to the level of detail as represented in the PDMM. Therefore, as a basic form of model validation, we compared important general patterns in the structure of the model community used in this study, which emerged from the assembly algorithm of the PDMM, with those of real marine communities; data from the Northeast Atlantic was used where possible. Specifically, we compared the body size range for phytoplankton species, the body size range for fish species, the trophic level range for fish species, phytoplankton species richness, fish species richness and the average dietary diversity for fish species (average number of species consumed by a fish species; Rossberg et al. 2011). Together, these properties have major effects on energy flow and competition patterns; thus, it is expected that reproducing them in the model is important for generating system dynamics similar to that of real communities. A minimum maturation body mass of $10^{-3.66}$ kg was

set for model fish species, which corresponds to the smallest size observed in the Celtic-Biscay Shelf and North Sea; this was derived by applying length-weight conversion parameters from FishBase (Froese & Pauly 2010) to maturation lengths for all fish species in these 2 regions. The lists of all fish species for the 2 regions were produced using the 'Information by Ecosystem' tool and 'All fishes' option at www.fishbase.org (Froese & Pauly 2010). Thus, the 5 indicators considered in this study were computed using model species with a maturation body size above $10^{-3.66}$ kg. Smaller model species were assigned the role of phytoplankton or non-fish consumer species, depending on trophic level.

Assurance that the dynamics of community size-structure predicted by the PDMM are close to those of real systems comes from our modelling results presented in Shephard et al. (2012). With the parameterisation described above, and under a fishing regime corresponding to that for the Celtic Sea between 1986 and 2004, the PDMM produces LFI and LSI time-series that closely match those observed for the Celtic Sea in this period (Shephard et al. 2012).

Fishing regimes applied

We examined community dynamics by conducting numerical experiments applying different fishing regimes (1 fishing regime per experiment) to the PDMM community. These regimes differed by (1) the size range of species fished, (2) the intensity of fishing and (3) the length of time over which fishing was imposed:

(1) For size-selectivity, either fish species across all sizes or just large fish species (defined as in the definition of the LSI) experienced fishing mortality. The former represents non-selective trawling (Piet et al. 2009) whereas the latter represents targeting of large fish species (Pauly et al. 1998). These regimes are analogous to those modelled by Andersen & Pedersen (2010).

(2) Fishing intensity is parameterised in terms of the harvesting rate H (yr^{-1}) of fished species, defined as the rate at which a population's total biomass decreases because of removals by fishing (as in Shephard et al. 2012). Harvesting rate is numerically comparable to the fishing mortality rate F, but more appropriate for the model structure of the PDMM. For 142 pairs of annual values of F and H for 8 assessed Celtic Sea fish species, the median F/H ratio was 1.21 (Shephard et al. 2012). A constant harvesting rate H was applied to each model fish species experiencing fishing mortality, for each experimental treatment. While this is a simplification of real exploitation patterns, it is consistent with the lack of size-dependence of H seen in empirical data: using data for 8 main demersal fish species in the Celtic Sea (*Gadus morhua*, *Lepidorhombus whiffiagoni*, *Lophius budegassa*, *L. piscatorius*, *Melanogrammus aeglefinus*, *Merlangius merlangus*, *Merluccius merluccius*, *Micromesistius poutassou*), we found only low correlations between $\log_{10}(H)$ and $\log_{10}$(maturation body mass) for each of the years 1986 to 2004, with all but one correlation found to be statistically indistinguishable from zero (Pearson's r of −0.066 to 0.420, such that $r^2 < 0.18$; the Shapiro-Wilk test gave $p > 0.05$ for all variables in each year apart from 1999, allowing normal distributions to be assumed in all years apart from 1999 — subsequently, *t*-tests were applied to test for significance of r, which gave $p > 0.05$ for all years except 1999). Here, H values were derived using data from ICES (2006, 2007, 2008, 2009, 2010), whereas maturation body masses were derived using FishBase (Froese & Pauly 2010), as described in 'Model validation' above. Similarly, empirical data for 6 main species in the North Sea (*G. morhua*, *M. aeglefinus*, *M. merlangus*, *Pollachius virens*, *Solea solea*, *Trisopterus esmarkii*) gave a low correlation for 17 out of 23 years spanning 1986 to 2008, with all 17 correlations found to be statistically indistinguishable from zero (Pearson's r of −0.010 to 0.523, such that $r^2 < 0.28$; the Shapiro-Wilk test gave $p > 0.05$ for all variables in each of the 17 yr and the *t*-test applied to r also gave $p > 0.05$ for each of these years). Here, H values were derived using data from ICES (2010) and maturation body masses were derived using FishBase (Froese & Pauly 2010), as described in 'Model validation' above. In addition, the baseline case where H is constant through time was investigated for each experimental treatment, to form a solid foundation against which results from more complex fishing regimes can be compared in future studies.

Five harvesting rates, H, were examined: 0.1 yr^{-1}, 0.2 yr^{-1}, 0.3 yr^{-1}, 0.4 yr^{-1} and 0.5 yr^{-1}. These values encompass a realistic range — using the empirical annual H values considered above together with total stock biomass estimates (ICES 2006, 2007, 2008, 2009, 2010), the biomass-weighted mean annual H for the Celtic Sea and North Sea ranges from 0.065 to 0.376 yr^{-1}.

(3) We examined the effects of fishing for durations of 25 and 50 yr — 25 yr is the approximate timescale over which LFI has declined from reference to low levels in the North Sea, following more than half a century at the reference level (Greenstreet et al.

2011). We examined 50 yr of fishing to see how more prolonged fishing affected recovery.

The 20 fishing regimes examined consisted of all combinations of the different fishing size-selectivities, intensities and durations. The dynamics of the 5 chosen indicators were tracked during the application of each fishing regime to the PDMM community. After simulation of each fishing regime, the indicator dynamics were tracked for a further 1000 yr in the absence of fishing, which gave sufficient time for each indicator to reach equilibrium (<0.1% change over last 100 yr). While the prohibition of fishing is not necessarily a realistic scenario, it provides a baseline for comparison with recovery scenarios that do have fishing pressure (Froese & Proelß 2010).

To aid interpretation of the indicator time-series, an increasing power-law saturating function was fitted to each, using non-linear least-square algorithms (R Development Core Team 2010):

$$I(t) = I_r\left(\frac{(t-t_f)^A}{(t-t_f)^A + B^A}\right) + I_f \quad (1)$$

where $I(t)$ is the value of an indicator at time t (measured from when fishing started), t_f is the time at which fishing stopped, I_f is the value of the indicator at t_f, and I_r, A and B are constants to be fitted. I_r represents the amount by which the indicator can recover after fishing is stopped, which is equivalent to the final equilibrium value of I reached during recovery minus I_f. The fitted power-law functions allowed recovery times to be calculated as a function of the remaining distance from equilibrium.

Model LFI was calculated using a large fish length threshold of 50 cm, whereas model LSI was calculated using a large species maximum length threshold of 85 cm. These thresholds have previously been found to give good sensitivity of the indicators to fishing for the Celtic Sea demersal fish community, relative to environmental factors (Shephard et al. 2011, 2012). The model $\bar{L}_{max}$ was calculated using the biomasses of model fish species and the maximum lengths of model fish species, derived from their maturation body masses using an empirical equation (Shephard et al. 2012). In order to calculate $\bar{L}_{mat}$, the maximum lengths were converted to maturation lengths using 2 other empirical equations (Froese & Binohlan 2000). Details of how the model LFI and LSI were calculated using the specified thresholds and how the model length-based indicators were calculated, including all empirical equations used, are given in the Supplement. $\bar{L}_{max}$ and $\bar{L}_{mat}$ were measured in cm; B_{tot} in kg m^{-2}.

RESULTS

Validation of model community

Model assembly using the parameterised PDMM produced a model shelf community with 189 fish species; this richness is at the lower end of the empirical range (Table 1, Fig. 1). Of these 189 fish species, 88 are classified as large, according to a maximum length threshold of 85 cm (Fig. 1). Species in this

Table 1. Comparison of values of key community properties for the Population-Dynamical Matching Model (PDMM) community used in this study with those of real communities. M_{mat} = maturation body mass; LFI = Large Fish Indicator

Community property	Value(s) for PDMM community	Value(s) for real communities	Data source(s)	Location(s) pertaining to data source(s)
M_{mat} for phytoplankton (kg)	$10^{-13.9}$–$10^{-8.76}$	10^{-15}–$10^{-8.69}$	Beardall et al. (2009), Barnes et al. (2011)	North Sea, Irminger Sea, Benguela upwelling, Norwegian Sea, 5 unspecified locations in Atlantic Ocean
M_{mat} for fish (kg)	$10^{-3.66}$–$10^{2.51}$	$10^{-3.66}$–$10^{2.54}$	Froese & Pauly (2010)	Celtic-Biscay Shelf, North Sea
Trophic level for fish	2.21–4.82	2–4.53	Froese & Pauly (2010)	Celtic-Biscay Shelf, North Sea
Phytoplankton species richness	4,701	268–1700	Smith et al. (2005), Ojaveer et al. (2010)	142 natural and 239 experimental aquatic ecosystems, Baltic Sea
Fish species richness	189	192–314	Froese & Pauly (2010)	Celtic-Biscay Shelf, North Sea
Average dietary diversity for fish species	15	6–14	Rossberg et al. (2011)	North Sea, Eastern Bering Sea, Northwest Atlantic Shelf, Open North Atlantic, Open Tropical Atlantic, South China Sea
LFI	0.761	0.4	Shephard et al. (2011)	Celtic Sea

model community had body sizes spanning ranges observed for real marine communities (Table 1, Fig. 1). In addition, 184 out of all 189 (97%) fish species had trophic levels within the empirical range, with trophic levels for the remaining fish species being within 7% of the upper limit of the empirical range (Table 1, Fig. 1). The average dietary diversity of model fish species, counting all resource species that contribute more than 1% to the diet of a fish species (Rossberg et al. 2011), was similar to (i.e. within 1 of) the upper limit of the empirical range (Table 1).

The species richness of modelled phytoplankton was 4701 (Table 1, Fig. 1). This is nearly 3 times greater than the empirically estimated upper limit of 1700, taken from a study for the Baltic Sea (Ojaveer et al. 2010; Table 1). However, considerable uncertainty remains over the true diversity of phytoplankton species (Simon et al. 2009). A lack of morphologically distinct features and incomplete sampling may have left most phytoplankton species yet to be identified. For example, the diatom species *Skeletonema costatum sensu lato* was recently found to consist of 8 cryptic species (Sarno et al. 2005, Smayda 2011). Since this example is far from unusual, we may reasonably expect phytoplankton diversity to be of the order emerging from the model.

Furthermore, the LFI value from the PDMM community was higher than 0.4 (Table 1), the value of the proposed LFI reference level for the Celtic Sea demersal fish community (Shephard et al. 2011). Significantly, this LFI reference level was set using data from a fished marine community, despite evidence that an unfished community would have a substantially higher biomass of large fish species. Myers & Worm (2003) estimated that large predatory fish biomass for 13 marine systems (including 4 continental shelf systems) is currently only 10% of the level prior to industrialised fishing. For the North Sea, Jennings & Blanchard (2004) estimated that recent biomasses of large fish in the weight categories 4–16 kg and 16–66 kg are 97% and 99% lower, respectively, than expected in the absence of fishing. Thus, the PDMM fish community used in this study was accepted as representative of a fish community in an unfished temperate shelf system.

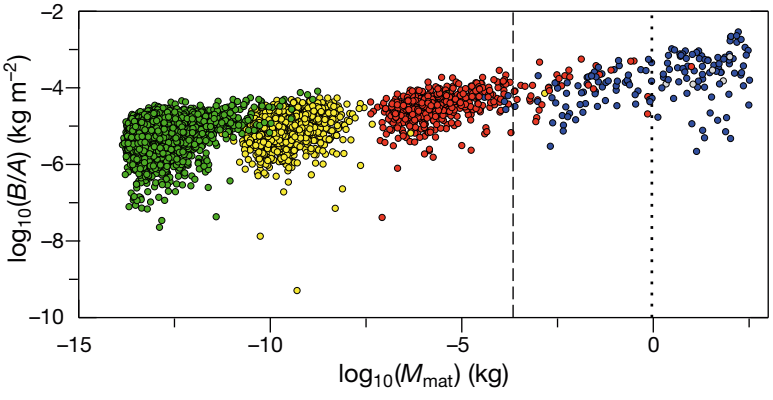

Fig. 1. Biomass density (biomass B divided by system area A) against maturation body mass (M_{mat}) for species in the Population-Dynamical Matching Model (PDMM) community used in this study. Each model species is represented by a dot, coloured to reflect its nearest integer-valued trophic level. Green, yellow, red, blue and grey correspond to trophic levels of 1, 2, 3, 4 and 5, respectively. The dashed and dotted vertical lines correspond to M_{mat} thresholds for a model fish species and a large model fish species respectively (see the Supplement at www.int-res.com/articles/suppl/m484p155_supp.pdf for how the M_{mat} threshold for a large model fish species was derived from a maximum length threshold of 85 cm)

Fish community dynamics under exploitation

The dynamics of the 4 indicators of community size-structure — LFI, LSI, $\bar{L}_{max}$ and $\bar{L}_{mat}$ — and the indicator of resource size, B_{tot}, exhibited similar trends during fisheries exploitation. Thus, only trends for the LSI are described in detail below, followed by a summary of results for the other 4 indicators. The LSI was chosen because it reflects the model structure of the PDMM better than the LFI, since model species are not resolved explicitly to the level of fish individuals, and unlike $\bar{L}_{max}$, $\bar{L}_{mat}$ and B_{tot}, LSI has been empirically found to be highly correlated with LFI (Shephard et al. 2012), which has been adopted by OSPAR and the EU for fisheries management (EU 2008, Heslenfeld & Enserink 2008, EC 2010, Greenstreet et al. 2011).

Fishing always reduced LSI, irrespective of size-selectivity, harvesting rate H or duration. The LSI was most sensitive to higher H (for H = 0.5 yr^{-1} relative to 0.1 yr^{-1}, increases of >0.46; Fig. 2), less sensitive to selective targeting of large fish species (for selective relative to non-selective fishing, increases of <0.06; Fig. 2) and least sensitive to a longer duration of fishing (for 50 relative to 25 yr of fishing, increases of <0.02; Fig. 2). For a given H, LSI was most sensitive to selective fishing on large fish species for 50 yr.

Since the LSI is the ratio of large fish species biomass to total fish biomass, it can decline as a result of a decrease in the biomass of large fish species or an increase in the biomass of small fish species. However, the model results show that the primary driver of declining LSI was loss of

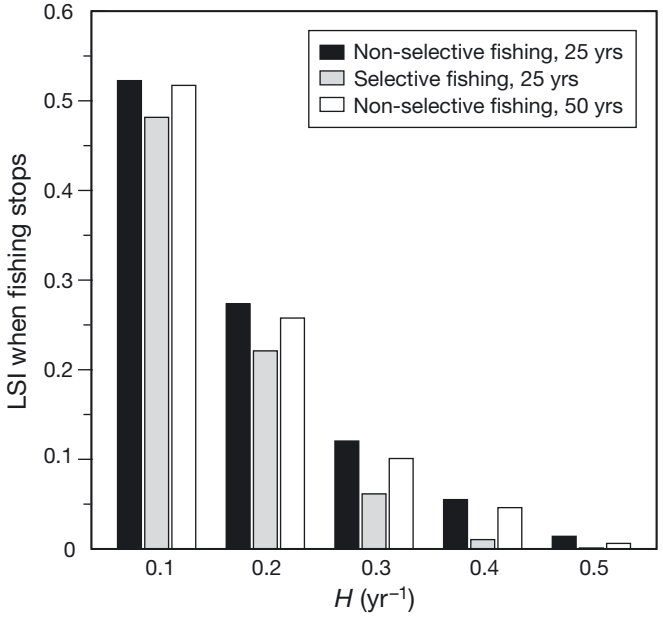

Fig. 2. Effects of higher harvesting rate (H) on Large Species Indicator (LSI) when fishing stops, for non-selective and selective fishing for 25 yr (difference in LSI <0.06 for all H tested), and non-selective fishing for 50 yr (compared with non-selective fishing for 25 yr, difference in LSI <0.02 for all H tested)

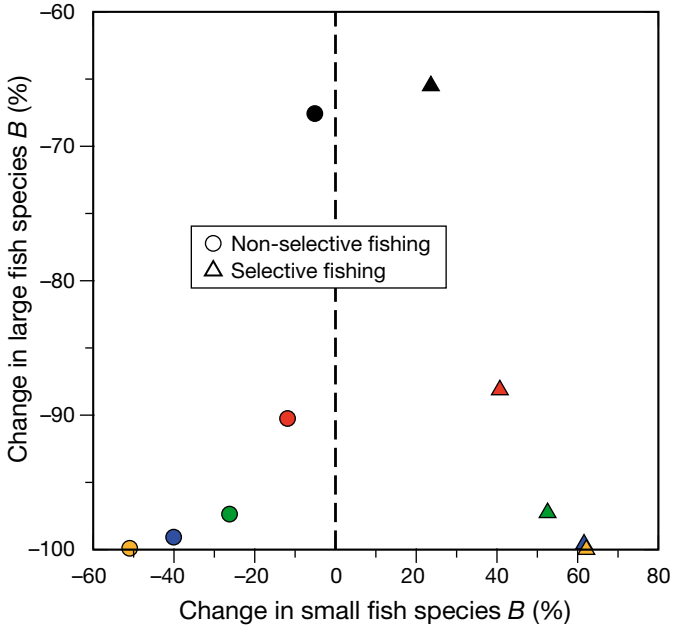

Fig. 3. Percentage change in large and small fish species biomass (B) after non-selective fishing (circles) or selective fishing of large fish species (triangles) for 50 yr. Black, red, green, blue and yellow represent harvesting rates (H) of 0.1, 0.2, 0.3, 0.4 and 0.5 yr^{-1} respectively. The dashed vertical line represents no change in small fish species biomass

biomass of large fish species, which exceeded 60% even with the lowest value of H tested (0.1 yr^{-1}; Fig. 3). For $H \geq 0.3$ yr^{-1}, the decline was very large (>95%; Fig. 3). The biomass of small fish species only increased under selective fishing; with $H \geq 0.4$ yr^{-1}, this type of fishing caused small fish species biomass to increase by >60%, reflecting a strong trophic cascade (Fig. 3). However, the percentage change in the biomass of small fish species was always less than the percentage change in the biomass of large fish species (Fig. 3).

The declining trends found for the LSI were also found for the 4 other indicators. Firstly, application of each of the 20 fishing regimes always led to a decline in each of the 4 indicators, with the primary driver being decreasing biomass of large fish species due to fishing. Secondly, each indicator was more sensitive to higher H than to a different size-selectivity or longer fishing duration; when H increased from 0.1 to 0.5 yr^{-1}, each indicator typically declined by >35% (Fig. 4). However, unlike the other 4 indicators including the LSI, B_{tot} was always higher when fishing was selective rather than non-selective.

Recovery of fish community size-structure

Once fishing ceased in the model, the 5 indicators measuring fish community size-structure and re-

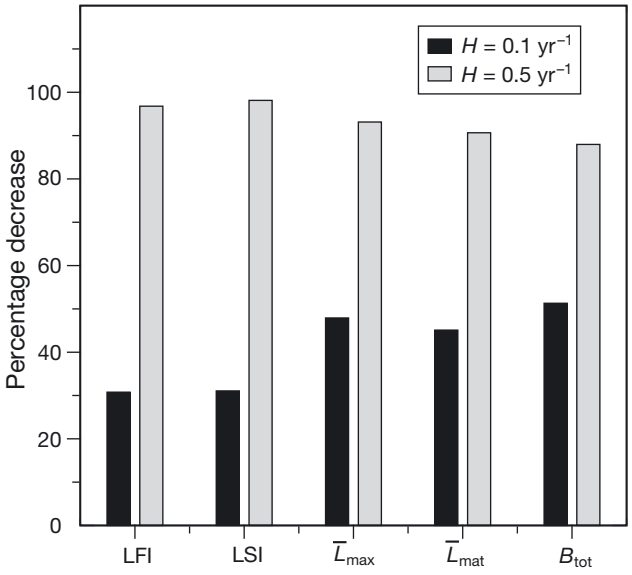

Fig. 4. Percentage decrease in Large Fish Indicator (LFI), Large Species Indicator (LSI), biomass-weighted mean maximum length of fish species ($\bar{L}_{max}$), biomass-weighted mean maturation length of fish species ($\bar{L}_{mat}$) and total fish biomass density (B_{tot}), after non-selective fishing for 25 yr at the minimum and maximum harvesting rates (H) tested

source size began to recover. Recovery is summarised by the final equilibrium level attained and the rate of reaching it. Since all 5 indicators exhibited similar trends in these 2 recovery measures, detailed results are presented only for the LSI; results for the other indicators are then briefly summarised.

After fishing at low harvesting rates ($H \leq 0.2$ yr^{-1}), subsequent cessation of fishing allowed full recovery of the LSI (Fig. 5), but higher H caused the final equilibrium level of LSI reached during recovery to fall below the pre-fishing baseline (Fig. 5). Under the highest tested harvesting rate of $H = 0.5$ yr^{-1}, the equilibrium LSI fell short of baseline by >60% when fishing lasted for 50 yr. When $H \geq 0.3$ yr^{-1}, a fishing duration of 50 yr resulted in lower recovery levels compared with 25 yr, by as much as >50% (Fig. 5). These trends were the same regardless of size-selectivity.

Local extinctions of large fish species mainly accounted for the long-term changes in LSI, and were more pronounced with higher H or a longer duration of fishing (Fig. 6a). Heaviest loss of large fish species richness occurred when fishing was long (50 yr) and intense ($H = 0.5$ yr^{-1}), where fewer than 10 of the 88 species remained with either non-selective or selective fishing (>88% decrease; Fig. 6a). In contrast, the richness of small fish species remained relatively insensitive to H or fishing duration, showing a decline from 101 to more than 70 (<30% decrease) even when fishing was long (50 yr) and intense ($H = 0.5$ yr^{-1}), regardless of selectivity type (Fig. 6b).

All 20 LSI recovery trajectories were well fit by the power-law saturating function of Eq. (1), with the coefficient of determination (R^2) ranging from 0.974 to 0.998. Fig. 7a shows the power-law fits for the 5 recovery trajectories after non-selective fishing for 25 yr, at the 5 different H values tested. For these trajectories, R^2 was lowest for $H = 0.5$ yr^{-1}, but was nonetheless very similar to R^2 values for the other H values (0.989 compared with 0.990–0.995 for $H = 0.1$ to 0.4 yr^{-1}). Furthermore, considering the 5 recovery trajectories after non-selective fishing for 50 yr; selective fishing for 25 yr; or selective fishing for

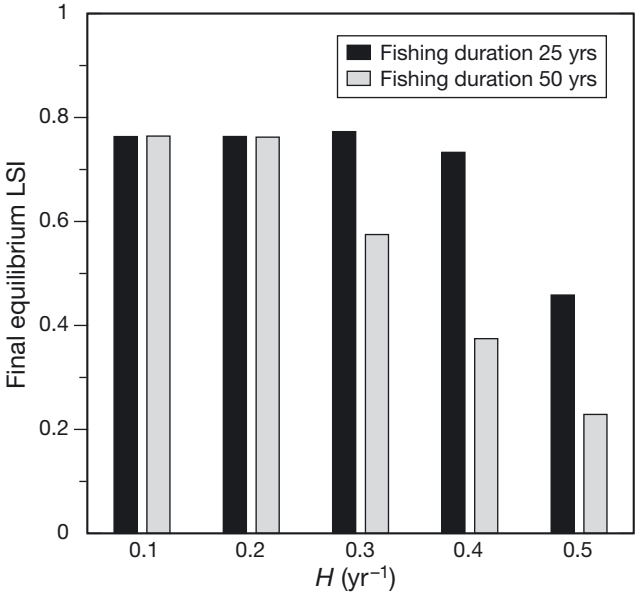

Fig. 5. Effects of higher harvesting rate (H) on Large Species Indicator (LSI) at equilibrium, after recovery from non-selective fishing lasting for 25 or 50 yr

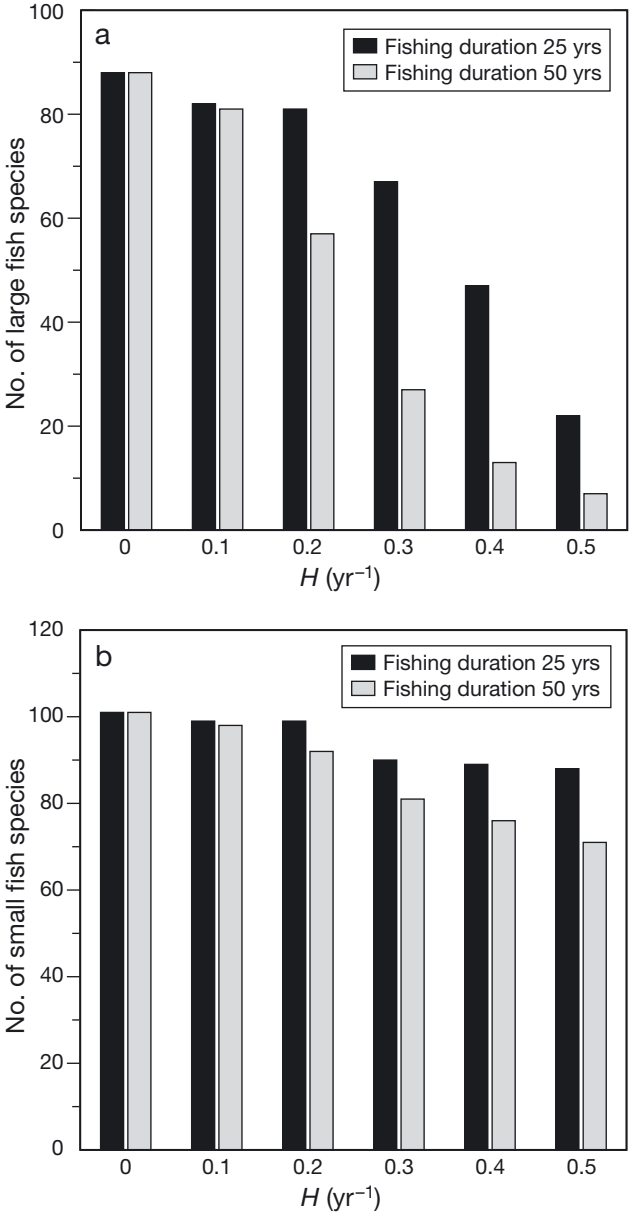

Fig. 6. Number of (a) large fish species and (b) small fish species at equilibrium, after recovery from non-selective fishing lasting for 25 or 50 yr

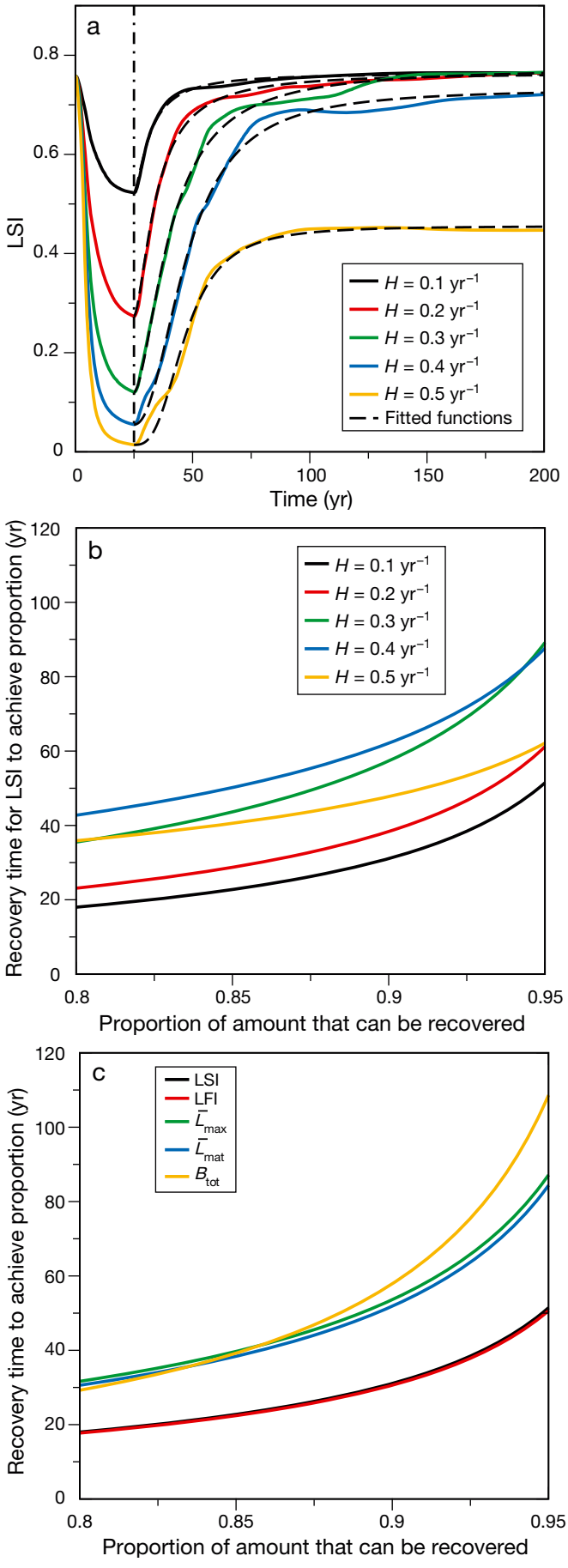

Fig. 7. (a) Large Species Indicator (LSI) recovery trajectories across different harvesting rates (H), after non-selective fishing for 25 yr. For each trajectory, a power-law function is fitted according to Eq. (1). Semi-dashed vertical line represents the time when fishing stops. (b) For each LSI trajectory in (a), times for recovery to near equilibrium, measured as times for recovery of 0.8 to 0.95 of the amount that can be recovered. These times are calculated from the fitted functions. (c) After non-selective fishing for 25 yr at $H = 0.1$ yr^{-1}, times for recovery to near equilibrium for the 5 indicators tested. All times are calculated from fitted power-law functions; the black line for the LSI is the same as that in (b). LFI = Large Fish Indicator; $\bar{L}_{max}$ = mean maximum length of fish species; $\bar{L}_{mat}$ = mean maturation length of fish species; B_{tot} = total fish biomass density

50 yr, R^2 was no longer lowest for $H = 0.5$ yr^{-1}. Thus, R^2 being lowest at $H = 0.5$ yr^{-1} for 25 yr of non-selective fishing is not part of a systematic trend.

In Eq. (1), the term in large brackets is equal to the proportion of LSI_r recovered. This equality can be rearranged to obtain the recovery time, $t - t_f$, as a function of the proportion of LSI_r recovered (Fig. 7b). These recovery time functions show that for recovery to near equilibrium, defined as 80 to 95% of LSI_r, multiple decades were usually required (Fig. 7b); for recovery to 95% of LSI_r, usually >50 yr and always >25 yr were required. Recovery time to near equilibrium generally increased with H. For example, after 25 yr of non-selective fishing at $H = 0.1$ yr^{-1}, the recovery time to 90% of LSI_r was 31 yr, but after 25 yr of non-selective fishing at $H = 0.2$, 0.3 and 0.4 yr^{-1} respectively, the recovery time increased to 38, 57 and 62 yr, respectively (Fig. 7b). This trend reflects fishing at higher H decreasing LSI at the end of the fishing period, which is LSI_f in Eq. (1), to a lower level. As a result, LSI_r, which represents the equilibrium LSI value reached during recovery minus LSI_f, increases. This means that the LSI needs to recover by a greater amount in order to reach near equilibrium, such that the corresponding recovery times tend to increase. For example, 25 yr of non-selective fishing at $H = 0.1$, 0.2, 0.3 and 0.4 yr^{-1} reduced LSI to 0.523, 0.273, 0.120 and 0.055, respectively (Fig. 2a), with the corresponding values of LSI_r being 0.240, 0.487, 0.647 and 0.678, respectively. An apparently contradictory reduction in recovery time with H was seen in some cases for high values of H. This was caused by large reductions in the equilibrium LSI reached during recovery at sufficiently high values of H, thus decreasing LSI_r and hence the recovery time. For example, after 25 yr of non-selective fishing at $H = 0.4$ and 0.5 yr^{-1}, the equilibrium LSI values reached during recovery were 0.733 and 0.458, respectively (Fig. 5), with the corresponding values of LSI_r being

0.678 and 0.454, respectively; the corresponding recovery times to 90% of LSI_r were 62 and 48 yr, respectively (Fig. 7b).

The other 4 indicators showed the same trends as the LSI. Firstly, full recovery was achieved for $H \leq 0.2$ yr^{-1}. Secondly, final equilibrium values decreased relative to the pre-fishing baseline for $H \geq 0.3$ yr^{-1}, the only exception being the case of 25 yr of fishing at $H = 0.3$ yr^{-1}; with 50 yr of fishing at $H = 0.5$ yr^{-1}, the equilibrium value fell short of baseline by >55%. Thirdly, for $H \geq 0.3$ yr^{-1}, a fishing regime lasting for 50 yr resulted in lower recovery levels relative to one lasting only 25 yr, by as much as >40%. All these trends were the same regardless of size-selectivity. Fourthly, the power-law saturating function of Eq. (1) gave good fits to the recovery trajectories, with R^2 ranging from 0.927 to 0.998 (see Fig. S5 in the Supplement for examples). The fitted power-law functions show that multiple decades were usually required for recovery to near equilibrium; for recovery to 95% of I_r, usually >50 yr and always >25 yr were required. In addition, recovery time generally increased with H.

Quantitatively, recovery times for the 5 indicators differed somewhat. Recovery times to near equilibrium for $\bar{L}_{max}$ and $\bar{L}_{mat}$ were usually greater than the corresponding times for both the LSI and LFI, often by >10 yr (Fig. 7c). Recovery times for B_{tot} were usually even longer than corresponding times for $\bar{L}_{max}$ and $\bar{L}_{mat}$ (Fig. 7c).

Examining mechanisms leading to slow recovery

The declining trends during fishing for all 5 indicators were found to be driven by reductions in the biomass of large fish species (Fig. 3). Thus, the slow recovery times found largely reflect slow realised population growth rates of large fish species. Because the maximum population growth rates of model species decrease with maturation body mass (Eq. S10 in the Supplement), small fish species in the model — together with smaller non-fish species — recover quickly relative to large fish species. Hence, food-limitation of large fish species is not a major mechanism leading to their slow realised population growth rates. The remaining possible mechanisms are predation of large fish species by small fish species and predation of large fish species by themselves. To measure the relative strengths of these mechanisms, the rates of predation of large fish species by the 2 groups of fish species were calculated for all 10 scenarios with 25 yr of fishing. The predation rate was calculated as the amount consumed divided by the biomass of large fish species, such that it measures predation pressure independent of resource availability. It was found that, during recovery, the rate of predation of large fish species by small fish species was usually much lower than the rate of predation of large fish species by large fish species. For all 10 scenarios and considering the first 100 yr of recovery, during which an indicator typically reached near equilibrium, the rate of predation of large fish species by large fish species was at least 200% greater than that by small fish species for the last 95 yr of this period — Fig. 8a shows results for the scenario with non-selective fishing for 25 yr at $H = 0.3$ yr^{-1}. These results demonstrate that predation of large fish species by large fish species is a much stronger mechanism underlying slow recovery than predation by small fish species.

However, the sharp initial increase in the predation of large fish species by themselves after fishing ceased (Fig. 8a), together with the negative correlation of the maximum population growth rate of a model fish species and its maturation body mass (Eq. S10 in the Supplement), suggests that among the large fish species, the relatively smaller species may recover quicker and thereby delay recovery of the larger species through increased predation. Therefore, we repeated the calculation of predation rates in Fig. 8a with a modified classification that only assigns the largest n fish species to the 'large' category and all other fish species to the 'small' category, where n is smaller than 88, the value corresponding to the original size threshold used in Fig. 8a (the same threshold as that used to define the LSI; see 'Materials and methods'). We tested n = 28, 48 and 68 and for each value, after fishing ceased, there was a pronounced increase in the rate of predation of 'large' fish species by 'small' fish species that lasted for multiple decades — the characteristic timescale for recovery of the 5 indicators examined. Fig. 8b shows results for n = 68.

DISCUSSION

Owing to the current and ongoing emphasis on the conservation of marine community size-structure in international fisheries management agreements (FAO 1995, EU 2008, 2010), we characterised a model marine community in terms of 4 indicators of community size-structure — the Large Fish Indicator (LFI), the Large Species Indicator (LSI), the biomass-weighted mean maximum length of fish species

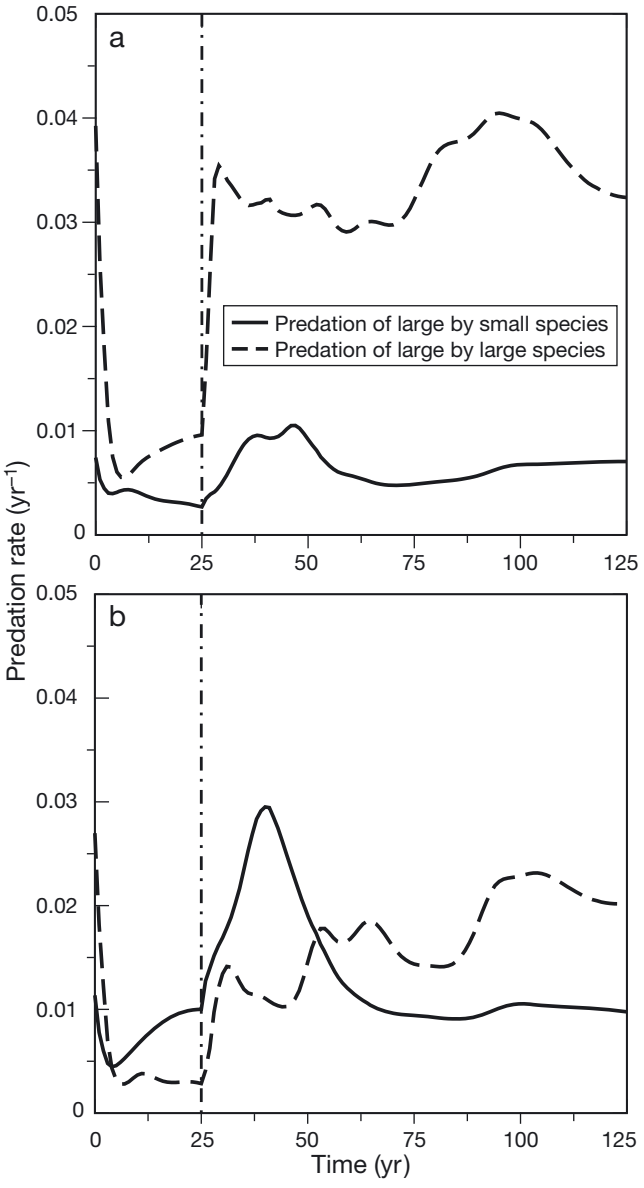

Fig. 8. (a) Rates of predation of large fish species by small fish species and by large fish species during non-selective fishing for 25 yr at a harvesting rate (H) of 0.3 yr^{-1}, and during 100 yr of recovery without fishing. There are 88 large and 101 small fish species, respectively. Semi-dashed vertical line represents the time when fishing stops. (b) Same as (a), except that the largest 68 fish species in the model community are taken as the 'large' fish species, with the 121 smaller fish species taken as the 'small' fish species

($\bar{L}_{max}$) and the biomass-weighted mean maturation length of fish species ($\bar{L}_{mat}$). In addition, we investigated one indicator of resource size, the total fish biomass density (B_{tot}), to complement the 4 size-structure indicators and offer a different perspective on community recovery. Dynamics of these 5 indicators were used to quantify the extent and rate of community recovery from fishing pressure, and it was found that all 5 indicators followed similar trends in our simulations. However, B_{tot} behaved in a qualitatively different way by being greater all the time under selective fishing of large fish species, relative to non-selective fishing; this was because of the greater biomass of (unfished) small fish species in the former scenario. This highlights a trade-off between managing for conservation of size-structure and managing for biomass production. There were also some noteworthy quantitative differences in recovery dynamics of the 5 indicators. B_{tot} tended to exhibit longer recovery times than $\bar{L}_{max}$ and $\bar{L}_{mat}$, which in turn usually had longer recovery times than the LSI and LFI, often by more than a decade. This demonstrates that changes in the precise mathematical form of indicators can lead to notable changes in recovery times. The LSI and LFI are both based on a biomass ratio, whereas $\bar{L}_{max}$ and $\bar{L}_{mat}$ are both based on a mean length; B_{tot} is a straightforward summation.

Overall, our results suggest substantial redundancy among the 4 size-structure indicators. However, although they all typically recover on multi-decadal timescales, the quantitative differences in recovery times between indicators suggest that different aspects of community size-structure can recover at considerably different rates. In addition, the results show that resource size typically takes a longer time to recover than community size-structure, suggesting that recovery of resource size could be predicated on prior recovery of size-structure to some extent.

The multi-decadal recovery times found in simulations, for the indicators examined, are corroborated by recent empirical studies of recovery in multi-species fish communities (Russ & Alcala 2010, Frank et al. 2011). For example, groundfish biomass in the eastern Scotian Shelf declined by >50% in the 1990s relative to the mid-1980s, and despite a 1993 moratorium on fishing cod and haddock, the size-structure of the groundfish community had not fully recovered by 2010 (Choi et al. 2004, Frank et al. 2011). In our simulations, the level of recovery in indicators after cessation of fishing was generally negatively correlated with both the intensity and duration of the fishing regime applied. For many scenarios tested, the indicators failed to reach a complete recovery at equilibrium due to local extinctions of large species, such that model community size-structure can recover to an equilibrium different than the pre-fishing one. On the eastern Scotian Shelf, the groundfish community may be settling to a new equilibrium size-structure following decreased fishing pressure, with much lower biomass of large predatory fish in comparison to the maximum recorded be-

fore their collapse (Frank et al. 2011). Thus, intense and/or prolonged fishing may result in cryptic erosion of recovery potential in the fish community.

In real systems, local extinctions may be reversed by immigration. This reversal can be demonstrated in the model we use if immigration is modelled in the form of a small constant biomass added to each fish species population every year (an immigration rate equivalent to 10^{-8} kg m^{-2} yr^{-1}, where 10^{-8} kg m^{-2} is equal to 1% of the smallest pre-fishing fish species population biomass density). After recovery from non-selective fishing for 50 yr at H = 0.3 yr^{-1}, there are only 6 local extinctions of large fish species, compared to 61 without immigration (Fig. 6a). In these simulations, populations that become locally extinct are assumed to be unable to re-establish by immigration from surrounding areas, possibly because of simultaneous local extinctions in these areas due to similar fishing regimes. As a result of the fewer number of extinctions, the final equilibrium LSI reached during recovery is lower than the pre-fishing value by <0.003, compared to 0.18 without immigration. However, the LSI value when fishing stops is similar to that in the case without immigration (difference of <0.001), as are recovery times to near equilibrium (differences of <6 yr). In addition, Dulvy et al. (2003) documented >50 local extinctions of marine fish populations worldwide, showing that prevention of local extinctions by immigration cannot be taken for granted. In particular, fish species with large body sizes (hence typically lower population growth rates) are more vulnerable to extinction (Dulvy et al. 2003). Our simulations concur and show much smaller extinction risk among fish species with small body sizes.

Changes in model indicator values were similar after fishing for 25 and 50 yr. This suggests that under sustained pressure from a new fishing regime, community size-structure attains near equilibrium within approximately 2 decades. The Celtic Sea demersal fish community may have provided a real example of this: the community-averaged fishing mortality increased sharply from 1977 to 1983 and fluctuated around a higher value during 1984 to 2008 (Shephard et al. 2011). Meanwhile, during 1986 to 2000, the LFI was lowered from a baseline of 0.5 to 0.1, around which the LFI has fluctuated until at least 2011 (Shephard et al. 2011, 2013). This suggests that steady fishing may have produced a new equilibrium state for the fish community, via a transient adjustment period of less than 20 yr (1984 to 2000). However, there is also evidence that environmental drivers such as changes in temperature have had an effect on the Celtic Sea demersal fish community size-structure (Blanchard et al. 2005); thus, further studies are required to determine the relative contributions of fishing and environmental drivers to changes in the Celtic Sea LFI. Furthermore, calculation of this LFI should be continued beyond 2011 to provide more robust evidence that a new equilibrium state has been reached.

All 5 indicators in all tested scenarios followed a power-law saturating function (Eq. 1), with only small fluctuations about this function. The smoothing responsible for such consistency is most likely due to the 'portfolio effect' already identified for richness-stability relationships (McCann 2000). This hypothesis is supported by a simulation using a smaller (dynamically stable) community of only 29 fish species, which produced stronger fluctuations about the power-law saturating function (Fig. 9). To produce this reduced community, a subset of the parameters (Table S1 in the Supplement) was changed to reduce the volume of the trophic niche space and hence the number of modelled species that appear during model assembly. Further details are given in the section on model parameterisation in the Supplement (in the subsection 'Scaling Biomasses of Modelled Populations'). The smoother recovery trajectories generated by the large model fish community for our main results are likely a better guide for real fish communities, because the model represents a realistic fish species richness of 189.

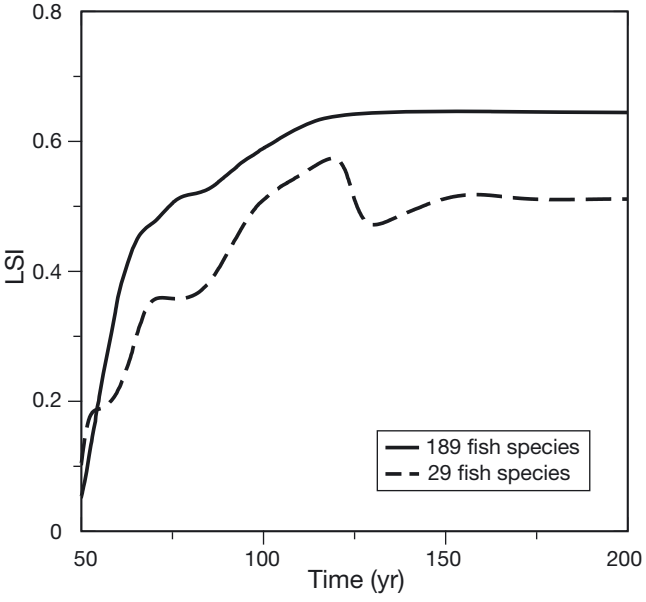

Fig. 9. Recovery trajectories after selective fishing of large fish species for 50 yr at a harvesting rate (H) of 0.3 yr^{-1}, for Population-Dynamical Matching Model (PDMM) communities with high (189) and low (29) fish species richness. LSI = Large Species Indicator

Mechanisms underlying indicator changes during fishing

Large fish species were substantially more vulnerable to fishing pressure than small fish species in our simulations, suffering more than 60% loss in biomass under non-selective (uniform) fishing pressure, while small fish species showed substantially smaller losses. The most likely explanation for this is the relatively slow population growth rate (Reynolds et al. 2005) of larger fish. Trophic cascades were also observed in our simulations, under selective fishing of large fish species. This observation is consistent with the cascades reported in the eastern Scotian Shelf and Black Sea fish communities (Frank et al. 2005, Daskalov et al. 2007), as well as those found by Andersen & Pedersen (2010) in their modelling study. However, our simulations indicate that trophic cascade effects are secondary in determining indicator dynamics, compared with the body size dependence of sensitivity to fishing among fish species.

Mechanisms causing slow recovery

The typically slow recovery of indicators found in our model simulations was attributable to slow recovery of large fish species. An explanation for such slow recovery of large fish species is juveniles of a subset of these large fish species suffering excess competition and/or predation from smaller fish species, which have been released by fishing from predation pressure by mature individuals of the subset of large species (Walters & Kitchell 2001, Fauchald 2010, Frank et al. 2011, Rossberg 2012). Our model exhibits the potential for such mechanisms to emerge, because it incorporates overlapping diet choices and mutual predation for 2 groups of fish species separated by a size threshold. Indeed, an examination of our simulation results revealed that the mechanisms were active during recovery, with the size threshold for separating the subset of large fish species ('large' fish species) and smaller fish species ('small' fish species) being larger than that used to calculate the LSI. A signature of the hypothesized mechanisms was clearly visible as an increase in the predation rate of 'large' fish species by 'small' fish species during recovery (Fig. 8b): 'small' fish species, released from predation, forage more intensively on 'large' fish species (i.e. on their juveniles) and hence delay recovery of the indicators examined.

Management implications

Marine conservation in the fisheries context is moving towards whole community management after many decades of concentration on individual species. The worldwide recognition of over-exploitation has led to various governmental commitments to restore fished populations, but the most prominent of these set targets for recovery of fish communities on timescales that seem unrealistic given our present findings. For example, the UN World Summit on Sustainable Development (WSSD; Johannesburg Plan of Implementation 2002) allowed just 13 yr to restore world fish stocks to levels producing MSY, and the EU Marine Strategy Framework Directive (MSFD; EU 2008) allowed just 12 yr for member states to restore the marine environment to 'good environmental status' (GES), with a proposed aspect of GES being fish community size-structure as measured by the LFI (EC 2010). Our simulations predict a wait of at least one, possibly several decades for management interventions to produce results that meet desired targets, and they also predict that in some cases we will find new stable size-structures that fall short of these targets. This is now exemplified by the North Sea demersal fish community, for which detailed LFI records have been calculated: LFI has fluctuated around 0.12 over 1990–2011 (Fung et al. 2012), despite reductions in the community-averaged fishing mortality since the late 1980s (Greenstreet et al. 2011). Recovery to the proposed reference value of 0.3 (corresponding to the GES milestone required by the MSFD; Greenstreet et al. 2011) appears unachievable within the next 8 yr. Similarly, the LFI for the Celtic Sea demersal fish community has fluctuated around 0.1 in the period 2000–2011, far from its proposed reference value of 0.4 (Shephard et al. 2011, 2013). On this basis, both of these fish communities in the North and Celtic Seas are unlikely to meet proposed MSFD targets.

Our results also show that in order to conserve fish community size-structure and maximise its recovery potential, measures aimed at conserving large fish species need to be integrated into fisheries management. In addition, recovery of fish community size-structure is more predictable if recovery trajectories have a common mathematical form, and our results provide evidence for this under the best-case recovery scenario of no fishing (Froese & Proelß 2010), when size-structure is measured by the LFI, LSI, $\bar{L}_{max}$ or $\bar{L}_{mat}$. Trajectories take the shape of a power-law saturating function, displaying a diminishing recovery rate with time since release from fishing pres-

sure. Interestingly, simulations with non-selective fishing (at H = 0.2, 0.3, 0.4 or 0.5 yr^{-1} for 25 or 50 yr) followed by limited non-selective fishing (H = 0.1 yr^{-1}) during the recovery period also exhibit LSI recovery trajectories that follow power-law saturating functions (R^2 ranging from 0.975 to 0.996). Moreover, in these simulations, recovery of LSI to near equilibrium still typically took multiple decades, even though the final equilibrium values are 0.04 to 0.25 smaller than corresponding values in the case of no fishing during recovery (Fig. 5). This demonstrates that the processes underlying slow recovery, as identified above, operate even when there is fishing during the recovery period: it appears that slow, saturating power-law recovery should be expected under a wide range of conservation management plans.

Lastly, size-selective fishing has been advocated to reduce discards of and impacts on bycatch species with important ecosystem roles (Pikitch et al. 2004), but this type of fishing may be detrimental to ecosystem structure by disproportionately targeting a subset of components (Zhou et al. 2010). Our model results indicate that 4 measures of fish community size-structure are affected by fishing principally through declines in the biomass of large fish species, rather than changes in the biomass of small fish species. Thus, recent proposals for 'balanced fishing' management strategies (Garcia et al. 2012) may help to preserve community size-structure predominantly by preventing disproportionate targeting of large fish species.

Acknowledgements. We thank 2 anonymous reviewers, whose comments and suggestions have resulted in significant improvements in this paper. T.F., K.D.F., D.G.R. and A.G.R. acknowledge funding from a Beaufort Marine Research Award, carried out under the *Sea Change* Strategy and the Strategy for Science Technology and Innovation (2006–2013), with the support of the Marine Institute, funded under the Marine Research Sub-Programme of the Irish National Development Plan 2007–2013. A.G.R. and S.S. acknowledge funding from the European Community's Seventh Framework Programme (FP7/2007–2013) under grant agreement MYFISH no. 289257. A.G.R. also acknowledges funding from the UK Department for Environment, Food and Rural Affairs (M1228).

LITERATURE CITED

Andersen KH, Beyer JE (2006) Asymptotic size determines species abundances in the marine size spectrum. Am Nat 168:54–61

Andersen KH, Pedersen M (2010) Damped trophic cascades driven by fishing in model marine ecosystems. Proc R Soc B 277:795–802

Andersen KP, Ursin E (1977) A multispecies extension to the Beverton and Holt theory of fishing, with accounts of phosphorus circulation and primary production. Meddelelser fra Danmarks Fiskeri- og Havundersøgelser 7: 319–435

Anderson TW (2001) Predator responses, prey refuges, and density-dependent mortality of a marine fish. Ecology 82: 245–257

Babcock RC, Shears NT, Alcala AC, Barrett NS and others (2010) Decadal trends in marine reserves reveal differential rates of change in direct and indirect effects. Proc Natl Acad Sci USA 107:18256–18261

Barnes C, Irigoien X, de Oliveira JAA, Maxwell D, Jennings S (2011) Predicting marine phytoplankton community size structure from empirical relationships with remotely sensed variables. J Plankton Res 33:13–24

Beardall J, Allen D, Bragg J, Finkel ZV and others (2009) Allometry and stoichiometry of unicellular, colonial and multicellular phytoplankton. New Phytol 181:295–309

Benoît E, Rochet MJ (2004) A continuous model of biomass size spectra governed by predation and the effects of fishing on them. J Theor Biol 226:9–21

Bersier LF, Kehrli P (2008) The signature of phylogenetic constraints on food-web structure. Ecol Complex 5: 132–139

Blanchard JL, Dulvy NK, Jennings S, Ellis JR and others (2005) Do climate and fishing influence size-based indicators of Celtic Sea fish community structure? ICES J Mar Sci 62:405–411

Blanchard JL, Jennings S, Law R, Castle MD and others (2009) How does abundance scale with body size in coupled size-structured food webs. J Anim Ecol 78: 270–280

Blanchard JL, Law R, Castle MD, Jennings S (2011) Coupled energy pathways and the resilience of size-structured food webs. Theor Ecol 4:289–300

Boudreau PR, Dickie LM (1992) Biomass spectra of aquatic ecosystems in relation to fisheries yield. Can J Fish Aquat Sci 49:1528–1538

Branch TA, Watson R, Fulton EA, Jennings S and others (2010) The trophic fingerprint of marine fisheries. Nature 468:431–435

Brown JH, Gillooly JF, Allen AP, Savage VM, West GB (2004) Toward a metabolic theory of ecology. Ecology 85: 1771–1789

Caldarelli G, Higgs PG, McKane AJ (1998) Modelling coevolution in multispecies communities. J Theor Biol 193:345–358

Cattin MF, Bersier LF, Banašek-Richter C, Baltensperger R, Gabriel JP (2004) Phylogenetic constraints and adaptation explain food-web structure. Nature 427: 835–839

Choi JS, Frank KT, Leggett WC, Drinkwater K (2004) Transition to an alternate state in a continental shelf ecosystem. Can J Fish Aquat Sci 61:505–510

Cury PM, Shannon LJ, Roux JP, Daskalov GM and others (2005) Trophodynamic indicators for an ecosystem approach to fisheries. ICES J Mar Sci 62:430–442

Daskalov GM, Grishin AN, Rodionov S, Mihneva V (2007) Trophic cascades triggered by overfishing reveal possible mechanisms of ecosystem regime shifts. Proc Natl Acad Sci USA 104:10518–10523

Department of Justice Canada (2005) Oceans Act: An Act respecting the oceans of Canada. Available at http://laws.justice.gc.ca/eng/acts/O-2.4/FullText.html

Drake JA (1990) The mechanics of community assembly and succession. J Theor Biol 147:213–233

Dulvy NK, Sadovy Y, Reynolds JD (2003) Extinction vulnerability in marine populations. Fish Fish 4:25–64

EC (2010) Commission decision of 1 September 2010 on criteria and methodological standards on good environmental status of marine waters. Official Journal of the European Union, 2010/477/EU

EU (2008) Establishing a framework for community action in the field of marine environmental policy (Marine Strategy Framework Directive). Official Journal of the European Union, 2008/56/EU

FAO (Food and Agriculture Organization) (1995) Code of Conduct for Responsible Fisheries. FAO, Rome

FAO (2003) Fisheries management 2. The ecosystem approach to fisheries. FAO technical guidelines for responsible fisheries 4, Suppl 2. FAO, Rome

Fauchald P (2010) Predator-prey reversal: A possible mechanism for ecosystem hysteresis in the North Sea? Ecology 91:2191–2197

Frank KT, Petrie B, Choi JS, Leggett WC (2005) Trophic cascades in a formerly cod-dominated ecosystem. Science 308:1621–1623

Frank KT, Petrie B, Fisher JAD, Leggett WC (2011) Transient dynamics of an altered large marine ecosystem. Nature 477:86–89

Froese R, Binohlan C (2000) Empirical relationships to estimate asymptotic length, length at first maturity and length at maximum yield per recruit in fishes, with a simple method to evaluate length frequency data. J Fish Biol 56:758–773

Froese R, Pauly D (2010) FishBase (09/2010). www.fishbase.org

Froese R, Proelß A (2010) Rebuilding fish stocks no later than 2015: Will Europe meet the deadline? Fish Fish 11:194–202

Fung T, Farnsworth KD, Reid DG, Rossberg AG (2012) Recent data suggest no further recovery in North Sea Large Fish Indicator. ICES J Mar Sci 69:235–239

Garcia SM, Kolding J, Rice J, Rochet MJ and others (2012) Reconsidering the consequences of selective fisheries. Science 335:1045–1047

Greenstreet SPR, Rogers SI (2006) Indicators of the health of the North Sea fish community: identifying reference levels for an ecosystem approach to management. ICES J Mar Sci 63:573–593

Greenstreet SPR, Rogers SI, Rice JC, Piet GJ and others (2011) Development of the EcoQO for the North Sea fish community. ICES J Mar Sci 68:1–11

Hall SJ, Collie JS, Duplisea DE, Jennings S and others (2006) A length-based multispecies model for evaluating community responses to fishing. Can J Fish Aquat Sci 63: 1344–1359

Halpern BS, Walbridge S, Selkoe KA, Kappel CV and others (2008) A global map of human impact on marine ecosystems. Science 319:948–952

Hartvig M, Andersen KH, Beyer JE (2011) Food web framework for size-structured populations. J Theor Biol 272: 113–122

Heslenfeld P, Enserink EL (2008) OSPAR Ecological Quality Objectives: the utility of health indicators for the North Sea. ICES J Mar Sci 65:1392–1397

Houle JE, Farnsworth KD, Rossberg AG, Reid DG (2012) Assessing the sensitivity and specificity of fish community indicators to management action. Can J Fish Aquat Sci 69:1065–1079

ICES (2006) Report of the working group on the assessment of southern shelf stocks of hake, monk and megrim (WGHMM). ICES CM 2006/ACFM:29

ICES (2007) Report of the working group on northern pelagic and blue whiting fisheries (WGNPBW). ICES CM 2007/ACFM:29

ICES (2008) Report of the working group on the assessment of southern shelf demersal stocks (WGSSDS). ICES CM 2008/ACOM:12

ICES (2009) Report of the working group on the assessment of southern shelf stocks of hake, monk and megrim (WGHMM). ICES CM 2009/ACOM:08

ICES (2010) Report of the working group on the assessment of demersal stocks in the North Sea and Skagerrak (WGNSSK). ICES CM 2010/ACOM:13

Jackson JBC, Kirby MX, Berger WH, Bjorndal KA and others (2001) Historical overfishing and the recent collapse of coastal ecosystems. Science 293:629–637

Jennings S, Blanchard J (2004) Fish abundance with no fishing: predictions based on macroecological theory. J Anim Ecol 73:632–642

Jennings S, Greenstreet SPR, Reynolds JD (1999) Structural change in an exploited fish community: a consequence of differential fishing effects on species with contrasting life histories. J Anim Ecol 68:617–627

Jennings S, Pinnegar JK, Polunin NVC, Boon TW (2001) Weak cross-species relationships between body size and trophic level belie powerful size-based trophic structuring in fish communities. J Anim Ecol 70:934–944

Jennings S, Pinnegar JK, Polunin NVC, Warr KJ (2002) Linking size-based and trophic analyses of benthic community structure. Mar Ecol Prog Ser 226:77–85

Jeschke JM, Kopp M, Tollrian R (2004) Consumer-food systems: why type I functional responses are exclusive to filter feeders. Biol Rev Camb Philos Soc 79: 337–349

Johannesburg Plan of Implementation (2002) Plan of implementation of the world summit on sustainable development, adopted at the world summit on sustainable development. UN, New York, NY

Law R, Morton RD (1996) Permanence and the assembly of ecological communities. Ecology 77:762–775

Loeuille N, Loreau M (2005) Evolutionary emergence of size-structured food webs. Proc Natl Acad Sci USA 102: 5761–5766

May RM (1977) Predators that switch. Nature 269:103–104

McCann KS (2000) The diversity-stability debate. Nature 405:228–233

Moustahfid H, Tyrrell MC, Link JS, Nye JA and others (2010) Functional feeding responses of piscivorous fishes from the northeast US continental shelf. Oecologia 163: 1059–1067

Murawski SA (2010) Rebuilding depleted fish stocks: the good, the bad, and, mostly, the ugly. ICES J Mar Sci 67: 1830–1840

Myers RA, Worm B (2003) Rapid worldwide depletion of predatory fish communities. Nature 423:280–283

Niklas KJ, Enquist BJ (2001) Invariant scaling relationships for interspecific plant biomass production rates and body size. Proc Natl Acad Sci USA 98:2922–2927

NOAA (2007) Magnuson-Stevens fishery conservation and management act: An Act to provide for the conservation and management of the fisheries, and for other purposes. Available at http://www.nmfs.noaa.gov/msa2005/docs/MSA_amended_msa%20_20070112_FINAL.pdf

Ojaveer H, Jaanus A, MacKenzie BR, Martin G and others (2010) Status of biodiversity in the Baltic Sea. PLoS ONE 5:e12467

Pauly D, Christensen V, Dalsgaard J, Froese R, Torres F (1998) Fishing down marine food webs. Science 279: 860–863

Pauly D, Christensen V, Guénette S, Pitcher TJ and others (2002) Towards sustainability in world fisheries. Nature 418:689–695

Piet GJ, van Hal R, Greenstreet SPR (2009) Modelling the direct impact of bottom trawling on the North Sea fish community to derive estimates of fishing mortality for non-target fish species. ICES J Mar Sci 66:1985–1998

Pikitch EK, Santora C, Babcock EA, Bakun A and others (2004) Ecosystem-based fishery management. Science 305:346–347

Plagányi EE (2007) Models for an ecosystem approach to fisheries. FAO Fish Tech Pap 477. FAO, Rome

Post WM, Pimm SL (1983) Community assembly and food web stability. Math Biosci 64:169–192

R Development Core Team (2010) R: a language and environment for statistical computing. R Foundation for Statistical Computing, Vienna

Reynolds JD, Dulvy NK, Goodwin NB, Hutchings JA (2005) Biology of extinction risk in marine fishes. Proc R Soc B 272:2337–2344

Rochet MJ, Benoît E (2012) Fishing destabilizes the biomass flow in the marine size spectrum. Proc R Soc B 279: 284–292

Rochet MJ, Trenkel VM (2003) Which community indicators can measure the impact of fishing? A review and proposals. Can J Fish Aquat Sci 60:86–99

Rochet MJ, Collie JS, Jennings S, Hall SJ (2011) Does selective fishing conserve community biodiversity? Predictions from a length-based multispecies model. Can J Fish Aquat Sci 68:469–486

Rossberg AG (2012) A complete analytic theory for structure and dynamics of populations and communities spanning wide ranges in body size. Adv Ecol Res 46:429–522

Rossberg AG, Matsuda H, Amemiya T, Itoh K (2006) Food webs: experts consuming families of experts. J Theor Biol 241:552–563

Rossberg AG, Ishii R, Amemiya T, Itoh K (2008) The top-down mechanism for body-mass–abundance scaling. Ecology 89:567–580

Rossberg AG, Brännström Å, Dieckmann U (2010) How trophic interaction strength depends on traits. Theor Ecol 3:13–24

Rossberg AG, Farnsworth KD, Satoh K, Pinnegar JK (2011) Universal power-law diet partitioning by marine fish and squid with surprising stability-diversity implications. Proc R Soc B 278:1617–1625

Russ GR, Alcala AC (2010) Decadal-scale rebuilding of predator biomass in Philippine marine reserves. Oecologia 163:1103–1106

Sarno D, Kooistra WHC, Medlin LK, Percopo I, Zingone A (2005) Diversity in the genus *Skeletonema* (Bacillariophyceae). II. An assessment of the taxonomy of *S. costatum*-like species with the description of four new species. J Phycol 41:151–176

Savage VM, Gillooly JF, Brown JH, West GB, Charnov EL (2004) Effects of body size and temperature on population growth. Am Nat 163:429–441

Scheffer M, Carpenter S, de Young B (2005) Cascading effects of overfishing marine systems. Trends Ecol Evol 20:579–581

Shephard S, Reid DG, Greenstreet SPR (2011) Interpreting the Large Fish Indicator for the Celtic Sea. ICES J Mar Sci 68:1963–1972

Shephard S, Fung T, Houle JE, Farnsworth KD and others (2012) Size-selective fishing drives species composition in the Celtic Sea. ICES J Mar Sci 69:223–234

Shephard S, Fung T, Rossberg AG, Farnsworth KD and others (2013) Modelling recovery of Celtic Sea demersal fish community size-structure. Fish Res 140:91–95

Shin YJ, Cury P (2004) Using an individual-based model of fish assemblages to study the response of size spectra to changes in fishing. Can J Fish Aquat Sci 61:414–431

Shin YJ, Rochet MJ, Jennings S, Field JG, Gislason H (2005) Using size-based indicators to evaluate the ecosystem effects of fishing. ICES J Mar Sci 62:384–396

Shin YJ, Shannon LJ, Bundy A, Coll M and others (2010) Using indicators for evaluating, comparing, and communicating the ecological status of exploited marine ecosystems. 2. Setting the scene. ICES J Mar Sci 67:692–716

Simon N, Cras AL, Foulon E, Lemée R (2009) Diversity and evolution of marine phytoplankton. C R Biol 332: 159–170

Smayda TJ (2011) Cryptic planktonic diatom challenges phytoplankton ecologists. Proc Natl Acad Sci USA 108: 4269–4270

Smith VH, Foster BL, Grover JP, Holt RD and others (2005) Phytoplankton species richness scales consistently from laboratory microcosms to the world's oceans. Proc Natl Acad Sci USA 102:4393–4396

Speirs DC, Guirey EJ, Gurney WSC, Heath MR (2010) A length-structured partial ecosystem model for cod in the North Sea. Fish Res 106:474–494

Taylor PJ (1989) Developmental versus morphological approaches to modelling ecological complexity. Oikos 55:434–436

Tremblay-Boyer L, Gascuel D, Watson, R, Christensen V, Pauly D (2011) Modelling the effects of fishing on the biomass of the world's oceans from 1950 to 2006. Mar Ecol Prog Ser 442:169–185

van Leeuwen E, Jansen VAA, Bright PW (2007) How population dynamics shape the functional response in a one-predator-two-prey system. Ecology 88:1571–1581

Walters C, Kitchell JF (2001) Cultivation/depensation effects on juvenile survival and recruitment: implications for the theory of fishing. Can J Fish Aquat Sci 58:39–50

Worm B, Hilborn R, Baum JK, Branch TA and others (2009) Rebuilding global fisheries. Science 325:578–585

Yoshida Y (2003) Dynamics of evolutionary patterns of clades in a food web system model. Ecol Res 18: 625–637

Zhou S, Smith ADM, Punt AE, Richardson AJ and others (2010) Ecosystem-based fisheries management requires a change to the selective fishing philosophy. Proc Natl Acad Sci USA 107:9485–9489

Editorial responsibility: Tim McClanahan, Mombasa, Kenya

Submitted: May 30, 2012; Accepted: February 6, 2013
Proofs received from author(s): May 6, 2013

The following supplement accompanies the article

Why the size structure of marine communities can require decades to recover from fishing

Tak Fung[1,*], Keith D. Farnsworth[1], Samuel Shephard[2], David G. Reid[3], Axel G. Rossberg[1,4]

[1]Queen's University Belfast, School of Biological Sciences, Belfast BT9 7BL, UK

[2]Marine and Freshwater Research Centre, Department of Life Sciences, Galway-Mayo Institute of Technology, Galway, Ireland

[3]Marine Institute, Fisheries Science Services, Rinville, Oranmore, Galway, Ireland

[4]Centre for Environment, Fisheries and Aquaculture Science (Cefas), Lowestoft, Suffolk NR33 0HT, UK

*Email: tfung01@qub.ac.uk

Marine Ecology Progress Series: 484: 155–171 (2013)

Supplement. This supplement details (1) the model structure, dynamics and underlying key assumptions for the PDMM (Population-Dynamical Matching Model) variant used in the main text; (2) the methodology used to parameterise the model; (3) details of how the 5 indicators used in the main text are calculated for the model community used; and (4) example recovery trajectories for 4 of the 5 indicators used, including power-law fits.

MODEL STRUCTURE AND DYNAMICS — FURTHER DETAILS

The Population-Dynamical Matching Model (PDMM) generates large model communities using an iterative process representing the natural assembly of complex ecological communities. For the PDMM variant used in the main text, the iterative assembly process is the same as that for the PDMM variant used in Rossberg et al. (2008), except for four differences: (1) only one community is modelled, as opposed to a metacommunity of 4 communities connected by migration; (2) more than 2 new species can appear in a modelled community in one iteration; (3) all trait values of model species are now constrained within defined boundaries (described in more detail below); and (4) a new formula for the functional response is used, incorporating a recent theory of prey-switching (described in more detail below). Hereafter, a summary of the iterative assembly process is given, followed by descriptions of details regarding the determination of trait values for newly invading species and the population dynamics of each model species. Throughout, there is particular focus on parts that differ from the PDMM variant used in Rossberg et al. (2008). Fig. S1 schematically illustrates the iterative assembly process, and Table S1 lists definitions for all model parameters used (Table S1 also gives the values derived for each parameter, and hence is found below after the section on 'Model Parameterisation').

Starting with an empty community, the first step in the iterative process is determination of the types (producer or consumer) and trait values of a small number of new species to be added to the community. The number of species added is $pS+1$ rounded down to the nearest integer, where S is the number of species currently in the community and p is a constant. When there are no extant producer species, the type of an invading species is automatically set to be a producer, because consumers can never invade in this case.

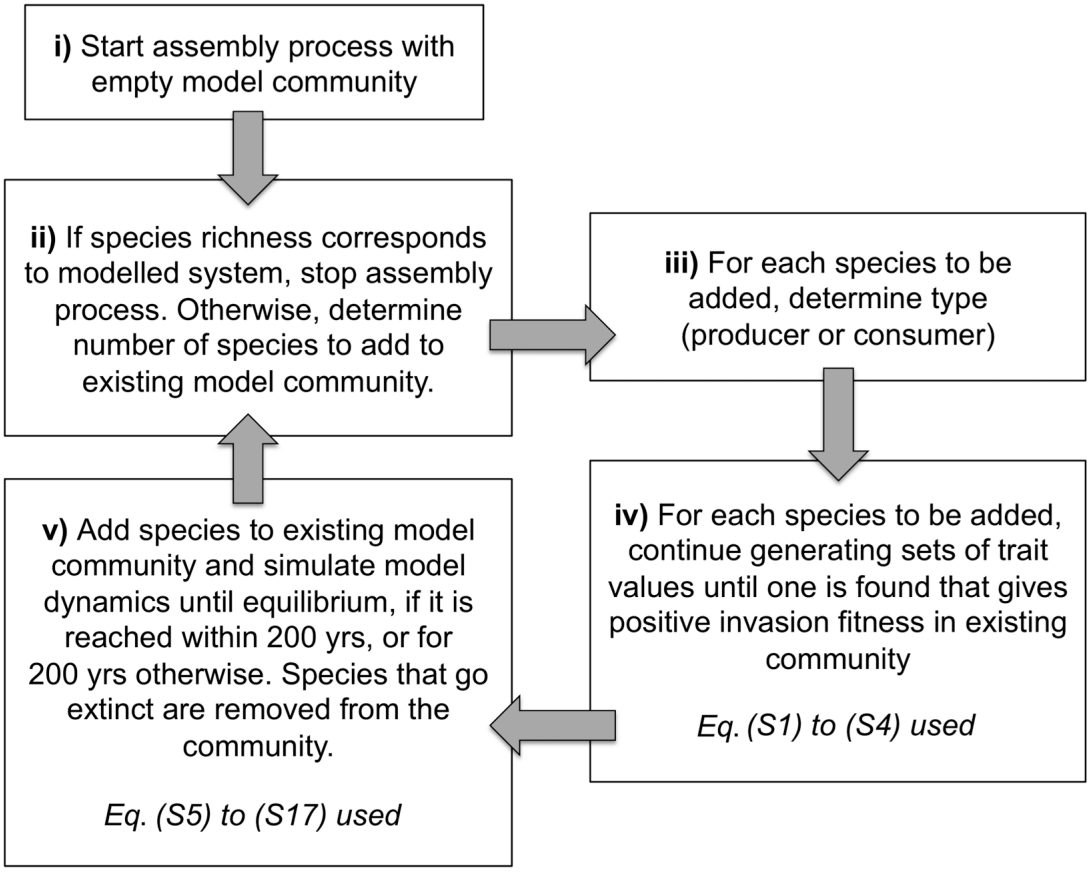

Fig S1. Schematic representation of the process by which the Population-Dynamical Matching Model (PDMM) generates a model community. Starting with an empty model community in Step i), an iterative loop, Steps ii)-v), is run repeatedly until the model community has species richness corresponding to the modelled system

Otherwise, the type of an invading species is determined by deciding at random with equal probability if it will be a producer or a consumer. Then, to determine the trait values of the invading species, an extant species of the same type is chosen at random and its traits modified, as described below, until one with a positive invasion fitness (Metz 2008) in the current community is found. This method of determining the trait values of invading species gives rise to phylogenetic correlations of traits, which have been empirically found to be important in structuring food-webs (Cattin et al. 2004, Bersier & Kehrli 2008, Naisbit et al. 2012). If there are no extant species of the same type as the invading species, then the body mass of the invading species is set to a default value and its other trait values are determined randomly, as described below.

After the types and trait values for all invading species have been determined, the set of invading species is then added to the community and population dynamics are simulated until the community reaches a dynamic equilibrium, where all populations have attained an equilibrium state. A heuristic algorithm is used at each time-step to determine whether this is the case, whereby, at a particular time-step, a species is taken to have reached an equilibrium if the natural logarithm of its population biomass has changed by <0.01 in the last third of the time-series simulated. In the uncommon situations where an equilibrium for the community cannot be detected after 200 yr of simulation time, the simulation is stopped at this point. Species that go extinct (species with population biomass smaller than maturation body mass, M_{mat}, or with an exponentially decaying population biomass) are removed from the model. An iteration ends after this simulation of the model dynamics. Once all iterations have been completed, if the final model community is not at a dynamic equilibrium, then model dynamics are simulated until one is reached.

Determination of Trait Values for New Species

For a new (invading) model species *k*, let $\vec{F}_k$, $\vec{G}_k$ and $\vec{V}_k$ be the vectors of foraging, (producer) competition and vulnerability traits respectively. The length of each vector, i.e. the number of quantitative traits it represents, is *D*. Contrary to the PDMM variant used by Rossberg et al. (2008), the value of each foraging, competition and vulnerability trait is now constrained such that it falls within a hypersphere of dimension *D* and radius r_F, r_G or r_V respectively. [A hypersphere is a sphere generalised to higher dimensions; specifically, a hypersphere of dimension $D \geq 4$ and radius *R* is the set of vectors $(x_1, x_2, \ldots, x_D)$ satisfying $x_1^2 + x_2^2 + \cdots + x_D^2 = R^2$.] Constraining the trait values to within hyperspheres effectively constrains the volume of trophic niche space, and hence the maximum number of species that can coexist in the model.

If there are no extant species of the same type as species *k*, then each trait vector is sampled from an even distribution of all trait vectors lying within the corresponding hypersphere. Otherwise, the trait values of species *k* are determined by mutating the trait values of a randomly chosen extant producer or consumer species *i*. The trait vectors for species *k* are given by:

$$\vec{F}_k = \vec{F}_i + \mu_F \vec{\xi} \qquad \text{(S1)}$$

$$\vec{G}_k = \vec{G}_i + \mu_G \vec{\xi} \qquad \text{(S2)}$$

and

$$\vec{V}_k = \vec{V}_i + \mu_V \vec{\xi} + \vec{V}_0 \qquad \text{(S3)}$$

where $\vec{\xi}$ represents a vector of random numbers that are independently sampled from a standard normal distribution, and μ_F, μ_G and μ_V determine the rates of change of the foraging, competition and vulnerability trait vectors, respectively. The vector $\vec{V}_0$ has as its first entry $s/2$ for producers and $-s/2$ for consumers, and all other entries equal to zero; the parameter *s* quantifies the separation of producers and consumers in their vulnerability traits (Rossberg et al. 2008). If the new trait value given by Eq. (S1), (S2) or (S3) falls outside the hypersphere with radius r_F, r_G or r_V, respectively (centred at 0 or, for vulnerability traits, at $\vec{V}_0$), then it is reflected back in at the surface of the hypersphere — for hypothetical neutral evolution, this leads to even distributions of traits in the hyperspheres.

If there are no extant species of the same type as species *k*, then the maturation body mass of the new species, $M_{\mathrm{mat},k}$, is set to the default value of 10^{-10} kg when species *k* is a producer and the default value of 10^{-7} kg when species *k* is a consumer. The default maturation body mass for consumers is the default value for producers multiplied by the preferred predator-prey M_mat ratio, $\eta_\mathrm{c} = 10^3$ (see section on 'Model Parameterisation' below). Otherwise, if an extant species of the same type as *k* exists, then $M_{\mathrm{mat},k}$ is obtained by mutating the maturation body mass of the selected ancestral species *i*, $M_{\mathrm{mat},i}$, according to:

$$M_{\mathrm{mat},k} = d^{\xi} M_{\mathrm{mat},i} \qquad \text{(S4)}$$

where ξ is a random number sampled from a standard normal distribution, so that $\log_e^2(d)$ becomes the variance of $\log_e\left(M_{\mathrm{mat},k}\right)$ in one time-step (Rossberg et al. 2008). If $M_{\mathrm{mat},k}$ is outside the range $\left[M_\mathrm{min}, M_\mathrm{max}\right]$, then the loss rate of the new species (see Eqs. S8 & S9 below) is increased by over an order of magnitude, which makes this species unviable.

Equations for Population Dynamics of Model Species

For a PDMM community with S species, which are indexed such that the S_p producer species come first, the equation describing the population biomass dynamics of a producer species i is:

$$\frac{\mathrm{d}B_i}{\mathrm{d}t} = \sigma_i \exp\left(-\sum_{j=1}^{S_\mathrm{p}} d_{ij}B_j\right)B_i - \sum_{j=S_\mathrm{p}+1}^{S} f_{ij}B_j - l_i B_i \qquad \text{(S5)}$$

where σ_i is the maximum population growth rate, d_{ij} is the competition coefficient for pro–ducer species i and j, f_{ij} is the functional response for prey species i and consumer species j, and l_i is the loss rate due to processes other than consumption. d_{ij} is a function of M_mat and the competition traits of species i and j; f_{ij} is a function of M_mat, the vulnerability traits of species i and the foraging traits of species j. The explicit forms of d_{ij} and f_{ij} are given in Eqs. (S11) & (S13) below.

The equation describing the population biomass dynamics of a consumer species i is:

$$\frac{\mathrm{d}B_i}{\mathrm{d}t} = \varepsilon\sum_{j=1}^{S} f_{ji}B_i - \sum_{j=S_\mathrm{p}+1}^{S} f_{ij}B_j - l_i B_i \qquad \text{(S6)}$$

where ε is the assimilation efficiency.

The maximum growth rate in Eq. (S5) and the loss rates in Eqs. (S5) & (S6) follow allometric scaling laws:

$$\sigma_i = C_\sigma M_{\mathrm{mat},i}^{\xi_\sigma} \qquad \text{(S7)}$$

$$l_{i,\mathrm{p}} = C_{l\mathrm{p}} M_{\mathrm{mat},i}^{\xi_{l\mathrm{p}}} \qquad \text{(S8)}$$

and

$$l_{i,\mathrm{c}} = C_{l\mathrm{c}} M_{\mathrm{mat},i}^{\xi_{l\mathrm{c}}} \qquad \text{(S9)}$$

where $l_{i,\mathrm{p}}$ and $l_{i,\mathrm{c}}$ are the loss rates, l_i, for producer and consumer species, respectively. An additional parameter determining the population dynamics of consumer species i is its maximum growth rate, $r_{i,\max}$. This is used to derive its handling time (Rossberg et al. 2008; see Eq. S15 for the explicit form of handling time), which is used in the formula for the functional response f_{ij} (see Eq. S13). $r_{i,\max}$ also follows an allometric scaling law:

$$r_{i,\max} = C_{r\max} M_{\mathrm{mat},i}^{\xi_{r\max}} \qquad \text{(S10)}$$

To model the physiological constraints that limit the maturation body sizes of organisms to lie above M_min, the loss rate is increased by $\left(\sigma_i - l_{i,\mathrm{p}}\right)\nu$ for producers and $\left(r_{i,\max} - l_{i,c}\right)\nu$ for consumers, where $\nu = 1\Big/\left[\left(M_\mathrm{mat}/M_\mathrm{min}\right) - 1\right]$. For the empirically-derived value of $M_\mathrm{min} = 10^{-15}$ kg (see next section on 'Model Parameterisation'), ν is very small (≤ 0.0101) if $M_\mathrm{mat} \geq 10^{-13}\,\mathrm{kg}$, so that the increase in the loss rate is negligible for all but the smallest species.

The explicit form of the producer competition coefficients d_{ij} is:

$$d_{ij} = d_{jj}\exp\left(-\frac{\left|\vec{G}_i - \vec{G}_j\right|^2}{2w_{\mathrm{p}}^2}\right) \tag{S11}$$

where the exponential term represents the niche overlap between the two producer species *i* and *j*, $\vec{G}$ is the competition trait vector and w_{p} is the producer niche width (Rossberg et al. 2008). In addition,

$$d_{jj} = \sigma_j \frac{\log_e\left(\sigma_j / l_{j,\mathrm{p}}\right)}{GPP_{\max} A} \tag{S12}$$

where $GPP_{\max}$ is the maximum gross primary production of a producer species in monoculture and A is the model area (Rossberg et al. 2008).

The formula for functional responses f_{ij} differs from that used by Rossberg et al. (2008). It is designed to give a more natural representation of prey-switching while preserving the "common sense condition" of Arditi & Michalski (1995) and Berryman et al. (1995): if a resource population is split into 2 populations with identical traits, then all dynamics are invariant (remain the same). This new form incorporates a theory of predator switching between multiple prey species (van Leeuwen et al. 2013) and is given by:

$$f_{ij} = \frac{a_j c_{ij} B_i \sum_{k=1}^{S} s_{ik} c_{kj} B_k}{\sum_{k=1}^{S} c_{kj} B_k \left(1 + a_j T_j \sum_{m=1}^{S} s_{km} c_{mj} B_m\right)} \tag{S13}$$

where a_j is the attack rate for consumer species *j*, T_j is the handling time for consumer species *j*, s_{ij} is the similarity between two prey species *i* and *j* with respect to prey switching, and c_{ij} is the trophic interaction coefficient for prey species *i* and consumer species *j*. Specifically, we used:

$$a_j = \frac{g l_{j,\mathrm{c}}}{A} \tag{S14}$$

where *g* is the aggressivity of consumer species,

$$T_j = \frac{\varepsilon}{r_{j,\max} + l_{j,\mathrm{c}}} \tag{S15}$$

as in Rossberg et al. (2008), and

$$s_{ij} = \exp\left(-\frac{\left|\vec{V}_i - \vec{V}_j\right|^2}{2w_{\mathrm{s}}^2}\right) \tag{S16}$$

where w_{s} is the switching similarity width, controlling the degree of prey switching. Unlike in the model variant of Rossberg et al. (2008), in Eq. (S14), the aggressivity *g* is fixed for all species following the model of Andersen & Pedersen (2010). This does not fundamentally change the model assembly procedure as the consumers still have different growth rates by virtue of their different traits, and accelerates model assembly.

The explicit form of c_{ij} has the same dependence on trophic traits as that given in the original formulation by Rossberg et al. (2008), but with a modified dependence on the predator-prey M_{mat} ratio. It is given by:

$$c_{ij} = \exp\left(-\frac{\left|\vec{F}_j - \vec{V}_i\right|^2}{2w_{\mathrm{c}}^2}\right)\left[\left(\frac{M_{\mathrm{mat},j}}{M_{\mathrm{mat},i}}\right)\left(\frac{1}{\eta_{\mathrm{c}}}\right)\right]^{-\alpha_{\mathrm{c}}} \quad \text{for } \frac{M_{\mathrm{mat},j}}{M_{\mathrm{mat},i}} > \eta_{\mathrm{c}} \qquad \text{(S17a)}$$

and

$$c_{ij} = \exp\left(-\frac{\left|\vec{F}_j - \vec{V}_i\right|^2}{2w_{\mathrm{c}}^2}\right)\left[\left(\frac{M_{\mathrm{mat},j}}{M_{\mathrm{mat},i}}\right)\left(\frac{1}{\eta_{\mathrm{c}}}\right)\right]^{\beta_{\mathrm{c}}} \quad \text{for } \frac{M_{\mathrm{mat},j}}{M_{\mathrm{mat},i}} \le \eta_{\mathrm{c}} \qquad \text{(S17b)}$$

where w_{c} is the consumer niche width and η_{c} is the preferred predator-prey M_{mat} ratio. α_{c} and β_{c} are exponents that determine how quickly the interaction strength c_{ij} decreases when the predator-prey M_{mat} ratio increases above and decreases below η_{c} respectively.

The functional response, Eq. (S13), can be derived by distinguishing for a predator species *j*, as in Holling's (1959) 'disk equation', those individuals that are currently handling prey and those that are actively foraging. However, differing from Holling, the propensity of the predator to consume prey *k* after having previously consumed prey *m* is scaled by a dimensionless factor s_{km} satisfying $s_{km} = s_{mk}$. Let B_{0k} be the biomass of predators belonging to species *j* that are not handling any prey and whose previous prey was species *k*, and let B_{km} be the biomass of predators belonging to species *j* that are handling prey species *k* and whose previous prey was species *m*. Then, following van Leeuwen et al. (2007, 2013), assuming that birth and death processes for the predator are slow compared to handling, since a predator handles many prey between births and deaths, gives:

$$\frac{\mathrm{d}B_{0k}}{\mathrm{d}t} = \sum_{m=1}^{S}\left(-a_j c_{mj} s_{mk} B_m B_{0k} + \frac{B_{km}}{T_j}\right) \qquad \text{(S18a)}$$

$$\frac{\mathrm{d}B_{km}}{\mathrm{d}t} = -\frac{B_{km}}{T_j} + a_j c_{kj} s_{km} B_k B_{0m} \qquad \text{(S18b)}$$

Assuming that these biomass components of predator species *j* are at equilibrium, so that we can set the right-hand sides in Eqs. (S18a,b) to 0, solving Eq. (S18b) for B_{km} and substituting into Eq. (S18a) gives:

$$\sum_{m=1}^{S}\left(-a_j c_{mj} s_{mk} B_m B_{0k} + a_j c_{kj} s_{km} B_k B_{0m}\right) = 0 \qquad \text{(S19)}$$

Eq. (S19) gives rise to a set of *S* equations with *S* unknowns $B_{01},\ldots,B_{0S}$. This system can be solved to give $B_{0m} = \lambda c_{mj} B_m$, where λ is a constant. The total biomass of predator species *j* is, using Eq. (S18b):

$$\sum_{k=1}^{S}\left(B_{0k} + \sum_{m=1}^{S} B_{km}\right) = \sum_{k=1}^{S}\left(B_{0k} + a_j T_j \sum_{m=1}^{S} s_{km} c_{kj} B_k B_{0m}\right) \qquad \text{(S20)}$$

whereas the biomass of prey species *i* consumed by attacking individuals of predator species *j* is

$$B_i \sum_{k=1}^{S} a_j c_{ij} s_{ik} B_{0k} \qquad \text{(S21)}$$

The functional response f_{ij} is the mean consumption rate of species j on species i, which is the expression in Eq. (S21) divided by the expression in Eq. (S20). This is equivalent to Eq. (S13).

MODEL PARAMETERISATION — FURTHER DETAILS

To fully specify the model, the rationale underlying the quantification of all model parameters is now described. After an explanation of the rationale for quantifying the parameter p, the detailed rationale for quantifying parameters related to the trait values of new species is given. This is followed by a discussion of the quantification of parameters related to population dynamics. The final part of this section shows how some of the model parameters can be changed to scale the biomass for each species in a PDMM community, such that results in the main text can be taken to be biomass-invariant.

Table S1 summarises the values used for all model parameters, together with data sources used for parameterisation. Methodologically, the parameterisation largely follows Rossberg et al. (2008), but a number of new data sources are used to achieve parameterisation of the model for a temperate marine shelf community. Wherever possible, data from the Northeast Atlantic is used.

Number of Invading Species

The parameter p, which determines the number of newly invading species per iteration, is chosen to be 0.01, as motivated by the need to ensure that model assembly is sufficiently quick while generally avoiding interactions between invading species.

Quantification of Parameters Used in Determination of Trait Values for New Species

The length of the trait vectors, D, is chosen to be 5, following Rossberg et al. (2008). In addition, the minimum maturation body mass, $M_{\min}$ is taken to be 10^{-15} kg, which is the lowest body mass found for marine phytoplankton from Beardall et al. (2009), assuming that 1 μm^3 is equivalent to 10^{-15} kg (Fenchel & Finlay 1983). The maximum maturation body mass, $M_{\max}$, is taken to be $10^{2.54}$ kg (347 kg), which is the highest maturation body mass calculated for fish species from the Celtic-Biscay Shelf and North Sea. These maturation body masses are calculated by applying length-weight conversion parameters from FishBase (Froese & Pauly 2010) to maturation lengths for all fish species in the two regions. The lists of all fish species for the two regions are produced using the 'Information by Ecosystem' tool and 'All fishes' option at www.fishbase.org (Froese & Pauly 2010).

For the other parameters used to determine trait values of new species, no directly measured empirical values are available. Thus, these parameters are adjusted freely to values (see Table S1) that give desirable model communities with properties resembling those for a temperate marine shelf community in the Northeast Atlantic (properties as described in 'Model validation' in the main text). In particular, the radius of the hypersphere constraining the values of the foraging traits, r_F, is fixed at a high value relative to the radius of the hypersphere constraining the values of the vulnerability traits, r_V (100 compared to 3.81). This means that the range of foraging traits of viable consumer species is limited and controlled by the range of vulnerability traits of viable resource species.

Quantification of Parameters Used in Equations for Population Dynamics of Model Species

In the dynamic equation for model consumer species, Eq. (S6), the assimilation efficiency, ε, is set to 0.6. This is the average of the 2 typical values for herbivores and carnivores taken from Hendriks (2007), derived by considering a range of invertebrates and vertebrates, including aquatic invertebrates and bony fish (Hendriks 1999).

The prefactors and exponents for the allometric scaling laws, Eq. (S7) to Eq. (S10), influencing population dynamics via Eqs. (S5) & (S6), are quantified as follows. For the scaling law used for the maximum population growth rate of producers, σ_i, the prefactor C_σ and exponent ζ_σ are set according to the empirical power-law of Niklas & Enquist (2001) for producers, including phytoplankton. For the scaling law used for the loss rate of producers, $l_{i,\mathrm{p}}$, the prefactor $C_{l\mathrm{p}}$ is set to the empirical value found by Brown et al. (2004) for unicellular eukaryotes and the exponent $\zeta_{l\mathrm{p}}$ is set to the theoretically derived, but empirically supported, value of –1/4 for biological organisms in general (Brown et al. 2004). Similarly, for the scaling law used for the loss rate of consumers, $l_{i,\mathrm{c}}$, the prefactor $C_{l\mathrm{c}}$ is set to the average of the 2 empirical values found by Brown et al. (2004) for fish and invertebrates, and the exponent is again set to –1/4 (Brown et al. 2004). For the scaling law used for the maximum growth rate of consumers, $r_{i,\max}$, the prefactor $C_{r\max}$ is difficult to quantify because in studies such as Hendriks (2007) and those used by Savage et al. (2004), the growth of organisms under conditions of maximum growth (no predators and a food supply that is not limiting) is not considered, or an approximation for $C_{r\max}$ is used that could lead to heavy underestimates for iteroparous species (May 1976) such as many marine fish and invertebrate species. In light of this uncertainty, $C_{r\max}$ is simply set to be a multiple of the prefactor for the loss rate, $C_{l\mathrm{c}}$, with the constant of proportionality chosen such that model consumer species can be generated with an M_{mat} range corresponding to that spanned by marine invertebrates and fish. The corresponding exponent $\zeta_{r\max}$ is set to the theoretically derived value of –1/4 (Savage et al. 2004). The precise values chosen for all prefactors and exponents are given in Table S1.

The parameters controlling the producer competition coefficients d_{ij}, given in Eq. (S11), are quantified as follows. Firstly, the producer niche width, w_{p}, is set freely in the absence of appropriate empirical data (as in Rossberg et al. 2008) to the value 1.32, which gives desirable model communities with properties resembling those for a temperate marine shelf community in the Northeast Atlantic (properties as described in 'Model validation' in the main text). Secondly, the maximum GPP of a single producer species, $GPP_{\max}$, is determined using primary production values from the Sea Around Us Project (2010) and the conversion relationship 1 g C = 1/0.07 g wet weight (Peters 1983). Using this data, the primary production of the North Sea is calculated as 5.81 kg m^{-2} yr^{-1} and that for the Celtic-Biscay Shelf is calculated as 4.99 kg m^{-2} yr^{-1}. Thus, $GPP_{\max}$ is set to a value, 0.131 kg m^{-2} yr^{-1}, that is below these 2 upper bounds and which gives producer species in the M_{mat} range for phytoplankton. Thirdly, the model area A is set to 5×10^{10} m^2, which is the area of the Celtic Sea as calculated using ICES rectangles (ICES 1977) and Vincenty's formulae (Vincenty 1975). However, as shown in the next section on Scaling Biomasses, model results can be taken to be invariant over a wide range of values of A spanning an order of magnitude.

Next, the parameters in the consumer functional response, Eq. (S13), are quantified. Firstly, as for w_{p}, the switching similarity width and the consumer niche width, w_{s} and w_{c} respectively, are set freely in the absence of appropriate empirical data to a value of 0.75. Similarly, the aggressivity for consumer species, g, is set freely in the absence of empirical data to $10^{5.51}$ kg^{-1} m^2. These choices give desirable model communities with properties

resembling those for a temperate marine shelf community in the Northeast Atlantic. Secondly, the preferred predator-prey M_{mat} ratio, η_{c}, is set to 10^3 following the analysis of Jennings et al. (2002) for a benthic fish and invertebrate community from the North Sea. Thirdly, the exponent that determines how quickly the interaction strength c_{ij} decreases when the predator-prey M_{mat} ratio increases above η_{c}, α_{c} (see Eq. S17a), is set to 0.05. This means that c_{ij} declines with an exponent of –0.05 above η_{c} (Fig. S2). Lastly, the exponent that determines how quickly the interaction strength c_{ij} decreases when the predator-prey M_{mat} ratio decreases below η_{c}, β_{c} (see Eq. S17b), is set to 0.25. This means that c_{ij} also decays below η_{c}, but quickly with an exponent of 0.25 (Fig. S2). These values of α_{c} and β_{c} are chosen to model the broad population-level predator-prey size windows resulting from the wide range of body sizes covered by typical marine organisms (Rossberg 2012, Section IX.C). For example, the larvae of cod (*Gadus morhua*) are about 0.4 cm long (Folkvord 2005) and feed on plankton (Mackinson & Daskalov 2008) that have small maturation body masses below about 10^{-8} kg (Beardall et al. 2009, Barnes et al. 2011); however, adult cod can grow to over 100 cm in length (Froese & Pauly 2010) and feed on fish that have maturation body masses above 10^{-1} kg, such as whiting (*Merlangius merlangus*) (diet of cod given by Mackinson & Daskalov [2008] and maturation body masses derived using data from FishBase [Froese & Pauly 2010], as described above). Thus, for cod, which has a maturation body mass of about 1 kg (derived using data from FishBase [Froese & Pauly 2010], as described above), the predator-prey mass ratio window spans more than 7 orders of magnitude. The window used in the PDMM decays exponentially below the preferred predator-prey ratio η_{c}, which means that a consumer's diet can contain species with larger maturation body masses, representing consumption of these larger species at early life-history stages. For example, small pelagic fish such as herring can feed upon the larvae of their larger predators (Walters & Kitchell 2001, Fauchald 2010). Thus, the wide predator-prey windows used in the PDMM capture competition between small and large species for food, as well as predation of small species on large species.

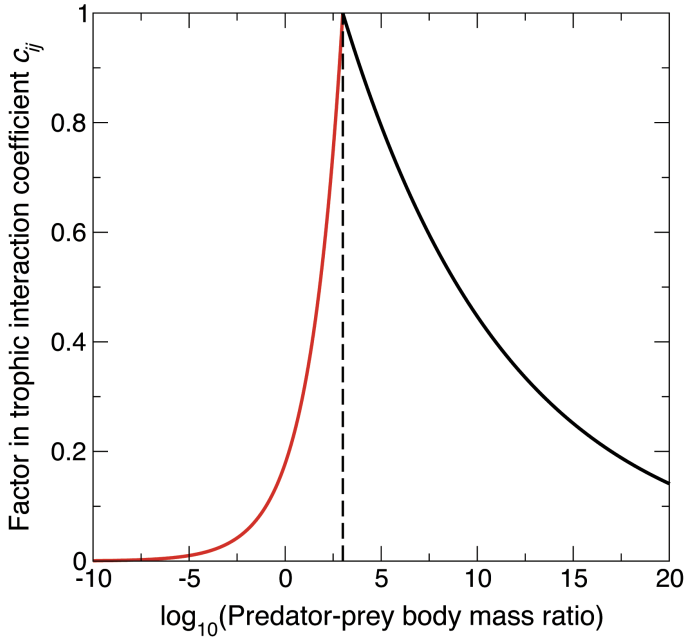

Fig. S2. Body-size dependence of the non-exponential factor in the model trophic interaction coefficient c_{ij}, for prey species with a smaller (black line; Eq. S17a) and larger (red line; Eq. S17b) maturation body mass than that corresponding to the preferred predator-prey M_{mat} ratio (dashed vertical line)

Scaling Biomasses of Modelled Populations

One of the PDMM parameters is the area modelled, A (see Table S1). It is easily verified from Eqs. (S5) to (S17) that, ignoring extinctions, model dynamics remain invariant when changing the value of A and scaling the population biomasses accordingly by a constant factor. Thus, changing A can only affect model dynamics by changing extinction times. However, for the large areas we consider, the biomass extinction threshold for each species is typically small relative to the biomass of any species in the model community, such that model dynamics should change by little with A (for example, species that take longer to go extinct when A is increased are expected to change model dynamics by little because their biomasses generally remain relatively small during the extended period). Therefore, changing A is expected to have little effect on model dynamics, and hence model assembly.

Nonetheless, we test the effects of using a range of A values covering the area of the Celtic Sea (approx. 5×10^{10} m^2; calculated using ICES rectangles (ICES 1977) and Vincenty's formulae from Vincenty 1975) to an area greater than that of the North Sea (approx. 7×10^{11} m^2; Sea Around Us Project 2010). Values for the other parameters are taken from Table S1, except for the radii of the hyperspheres for the foraging, competition and vulnerability traits (r_F, r_G, r_V); the parameters determining the variability of these traits (μ_F, μ_G, μ_V); and the producer-consumer separation (s). These seven parameters are multiplied by a factor of 2/3, such that the possible range of values that each foraging, competition and vulnerability trait can take is smaller, resulting in fewer model species and smaller model communities. Using these parameter values in the PDMM assembly procedure gave a model shelf community that grew in species richness, at similar rates over the range of A considered (Fig. S3). For each of the six A values tested, model assembly was run until about 24000 species were added to the existing community by invasion. At this point, it was clear that increasing A did not produce a systematic trend in the species richness trajectories. Thus, only one value of A was used to produce simulation results in the main text, the smallest value (Table S1). Note that the set of parameters used to draw the black line in Fig. S3, with the smallest value of A, was also used to generate the small model community used for Fig. 9 in the main text.

There is a second scaling transformation that leaves model dynamics essentially unchanged. Ignoring extinctions, from Eqs. (S5) to (S17), increasing the maximum GPP of a single producer species, GPP_{max}, and decreasing the aggressivity, g, by a constant factor X has the same effect as increasing A by the factor X, except that now both biomass density and biomass of each species increases by X. Thus, as for changing A, changing GPP_{max} and g in this way can only affect model dynamics by changing extinction times. However, as for changing A, model dynamics should change by little when rescaling GPP_{max} and g, because the biomass extinction threshold for each species is typically small relative to the biomass of any species in the model community. GPP_{max} can be varied up to 5.81 kg m^{-2} yr^{-1} (see details of its parameterisation in the section on 'Model Parameterisation' above; Sea Around Us Project 2010) and g can be varied in the absence of empirical data for its parameterisation. Thus, for the model community used in the main text, the biomass of each species can be scaled up or down by varying A or GPP_{max} and g, with little effect on model dynamics. Therefore, our results can be taken to hold if the biomass and/or biomass density of each species is scaled by a factor X, because model dynamics can be taken to be largely invariant in these cases.

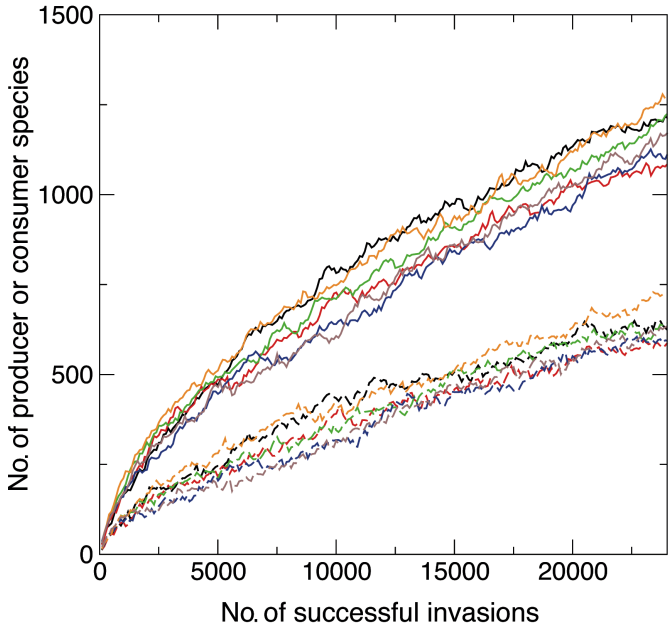

Fig. S3. Model assembly trajectories for parameter sets (see text in Supplementary Material for details) with different areas A, showing how the number of producer and consumer species (solid and dashed lines respectively) change with the number of species added to/invading the community. The black, red, green, blue, orange and brown lines represent increasing values of A being used: 5×10^{10} m^2, 1×10^{11} m^2, 2.5×10^{11} m^2, 5×10^{11} m^2, 7.5×10^{11} m^2 and 1×10^{12} m^2 respectively

Table S1. List of parameters in the Population-Dynamical Matching Model (PDMM) together with their definitions and values, and any data sources used for quantification

Parameter	Definition	Value	Data source(s)
Species invasion parameters			
d	Determines the amount by which M_{mat} for an existing species varies when determining M_{mat} for a new invading species. The new value of $\log_e\left(M_{\text{mat}}\right)$ is the old value plus a random normal variable with mean 0 and standard deviation $\log_e(d)$.	4	
D	Niche space dimension	5	Rossberg et al. (2008)
M_{min}	Minimum M_{mat} that a model species can take.	10^{-15} kg	Fenchel & Finlay (1983), Beardall et al. (2009)
M_{max}	Maximum M_{mat} that a model species can take.	$10^{2.54}$ kg	Froese & Pauly (2010)
p	$pS+1$ rounded down to the nearest integer is the number of species invading at each iteration.	0.01	
$r_{\text{F}}, r_{\text{G}}, r_{\text{V}}$	Radii of hyperspheres for the foraging traits (r_{F}), producer competition traits (r_{G}) and vulnerability traits (r_{V}).	100, 6.42, 3.81	
s	Producer-consumer trait separation	1.91	

μ_F, μ_G, μ_V	Determines the amount by which each of the foraging, competition and vulnerability trait values for an existing species varies when determining values for a new invading species. A new trait value is given by the old value plus a random normal variable with mean 0 and standard deviation μ_F (foraging traits), μ_G (competition traits) or μ_V (vulnerability traits).	1.2, 1.5, 1.05	
Model dynamics parameters			
A	Area modelled	5×10^{10} m^2	Vincenty (1975), ICES (1977)
g	Aggressivity	$10^{5.51}$ kg^{-1} m^2	
$C_{l\mathrm{c}}$	Prefactor for $l_{i,\mathrm{c}}$	0.298 kg$^{1/4}$ yr^{-1}	Brown et al. (2004)
$C_{l\mathrm{p}}$	Prefactor for $l_{i,\mathrm{p}}$	0.161 kg$^{1/4}$ yr^{-1}	Brown et al. (2004)
$C_{r\max}$	Prefactor for $r_{\max,i}$	$5C_{lc}$	
C_σ	Prefactor for σ_i	0.531 kg$^{1/4}$ yr^{-1}	Niklas & Enquist (2001)
$GPP_{\max}$	Maximum GPP of a single producer species	0.131 kg m^{-2} yr^{-1}	Peters (1983), Sea Around Us Project (2010)
w_c	Niche width for consumers	0.75	
w_p	Niche width for producers	1.32	

w_{s}	Switching similarity width	0.75	
α_{c}	Small prey exponent	0.05	
β_{c}	Big prey exponent	0.25	
η_{c}	Preferred predator-prey M_{mat} ratio	10^3	Jennings et al. (2002)
ε	Assimilation efficiency for consumers	0.6	Hendriks (2007)
$\zeta_{l\mathrm{c}}$	Allometric exponent for $l_{i,\mathrm{c}}$	–0.25	Brown et al. (2004)
$\zeta_{l\mathrm{p}}$	Allometric exponent for $l_{i,\mathrm{p}}$	–0.25	Brown et al. (2004)
$\zeta_{r\max}$	Allometric exponent for $r_{\max,i}$	–0.25	Savage et al. (2004)
ζ_{σ}	Allometric exponent for σ_i	–0.25	Niklas & Enquist (2001)

Calculation of Five Indicators for Model Community

The model Large Fish Indicator (LFI), using a 50 cm large fish length threshold, is calculated following Shephard et al. (2012). First, for each model fish species, the maturation body mass, M_{mat}, is converted to a corresponding L_{max} using the empirical equation (working in cm and kg) $\log_{10}(L_{max}) = 0.385 \times \log_{10}(M_{mat}) + 1.88$ ($r^2 = 0.640$; Fig. S4a). This equation was derived by performing a reduced major axis (RMA) regression on 91 pairs of $\log_{10}(M_{mat})$ and $\log_{10}(L_{max})$ values for 91 fish species from the West Coast Groundfish Survey (WCGFS) for the Celtic Sea. A RMA regression was used to account for uncertainty in both M_{mat} and L_{max}; this is an improvement over the linear regression used in Shephard et al. (2012), which only accounted for uncertainty in L_{max}.

Second, for each model fish species with $L_{max} > 50$ cm, the proportion of total species biomass due to individuals above 50 cm, α, is derived using the empirical equation $\alpha = 2.55 \times \log_{10}(L_{max}) - 4.32$ ($r^2 = 0.461$; Fig. S4b), with the value of α capped at 1, as required. This equation was derived by performing a RMA regression on 38 pairs of α and $\log_{10}(L_{max})$ values for 38 fish species from the WCGFS. This is an improvement over the non-linear regression used in Shephard et al. (2012), which only accounts for uncertainty in α. By definition, $\alpha = 0$ for model fish species with $L_{max} \leq 50$ cm. The model LFI is then easily calculated as the sum of the products of biomass and α for all model fish species divided by the biomass of all model fish species.

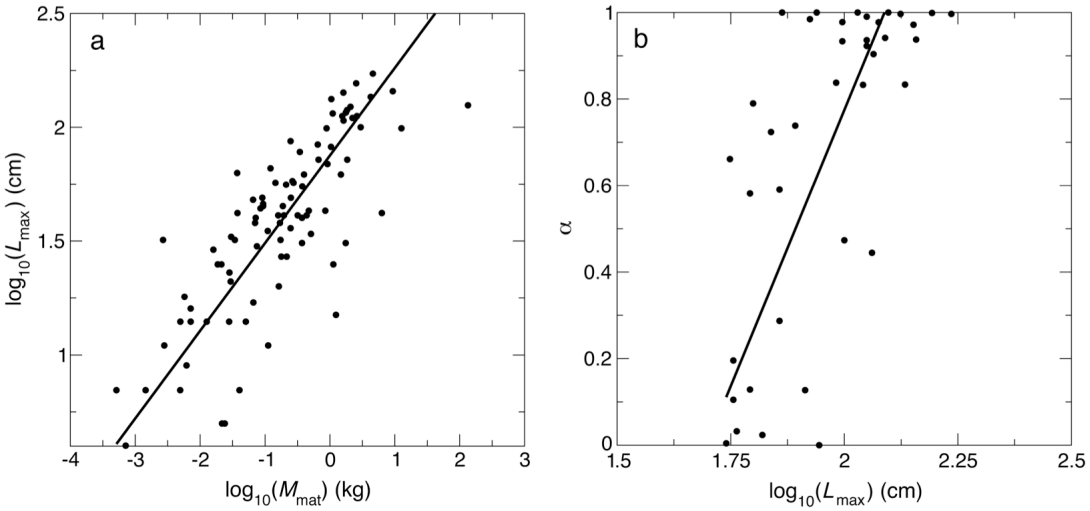

Fig. S4. (a) Relationship between maximum length, L_{max}, and maturation body mass, M_{mat}, derived using RMA regression (solid line) on data for 91 fish species from the West Coast Groundfish Survey (WCGFS) (filled circles). (b) Relationship between proportion of species biomass due to individuals above 50 cm, α, and L_{max}, derived using RMA regression (solid line) on data for 38 species from the WCGFS (filled circles). See text for equations and goodness of fits

The model Large Species Indicator (LSI), using an 85 cm large fish species maximum length threshold, is calculated following Shephard et al. (2012). First, the 85 cm L_{max} threshold is converted to an M_{mat} threshold of 1.38 kg using the empirical equation relating M_{mat} and L_{max} above (see also Fig. S4a). The model LSI is then simply the sum of the biomass of all model fish species with $M_{mat} > 1.38$ kg divided by the biomass of all model fish species.

The model biomass-weighted mean maximum length of fish species ($\overline{L}_{max}$) is calculated by first converting M_{mat} for each model fish species to the corresponding L_{max}, using the empirical equation relating M_{mat} and L_{max} above (see also Fig. S4a). The model $\overline{L}_{max}$ is then calculated as the biomass-weighted mean of all these L_{max} values.

To calculate the model biomass-weighted mean maturation length of fish species ($\overline{L}_{mat}$), L_{max} for each model fish species is first converted to a corresponding L_∞ using the empirical equation (working in cm) $\log_{10}(L_\infty) = 0.9841 \times \log_{10}(L_{max}) + 0.044$ ($n = 551$, $r^2 = 0.959$; Froese & Binohlan 2000). Subsequently, L_∞ for each model fish species is converted to a corresponding L_{mat} using the empirical equation (working in cm) $\log_{10}(L_{mat}) = 0.8979 \times \log_{10}(L_\infty) - 0.0782$ ($n = 467$, $r^2 = 0.888$; Froese & Binohlan 2000). Both these equations were derived from hundreds of recorded pairs of values of the regressed variables (Froese & Binohlan 2000). The model $\overline{L}_{mat}$ is then calculated as the biomass-weighted mean of all these L_{mat} values.

The total fish biomass density (B_{tot}) is calculated simply by summing up the biomasses of all model fish species, working in kg, and then dividing by the modelled area A (Table S1).

RECOVERY TRAJECTORIES — FURTHER EXAMPLES

Fig. S5a–d shows recovery trajectories for the LFI, the biomass-weighted mean maximum length of fish species ($\overline{L}_{max}$), the biomass-weighted mean maturation length of fish species ($\overline{L}_{mat}$) and the total fish biomass density (B_{tot}), respectively, after non-selective fishing for 25 yr at harvesting rates $H = 0.1$, 0.2, 0.3, 0.4 and 0.5 yr^{-1}. Power-law saturating functions fitted to the recovery trajectories (as described in main text), are also shown. These give extremely good fits, with R^2 ranging from 0.927 to 0.998. The saturating shape means that recovery becomes increasingly slow, resulting in slow recovery times to near equilibrium — usually multiple decades. Moreover, the common shape of the recovery trajectories for all indicators facilitates prediction for management. As for the LSI, for all indicators, R^2 was lowest for $H = 0.5$ yr^{-1}, but was nonetheless high and close to R^2 for the smaller H values. In addition, this trend was not found when considering selective fishing for 25 or 50 yr. Thus, there is no evidence of its general importance.

As described in the main text, recovery times to near equilibrium for B_{tot} were typically longer than that for both $\overline{L}_{max}$ and $\overline{L}_{mat}$, which in turn were usually longer than that for both the LSI and LFI. Longer recovery times are reflected by trajectories that take longer to saturate (Fig. S5).

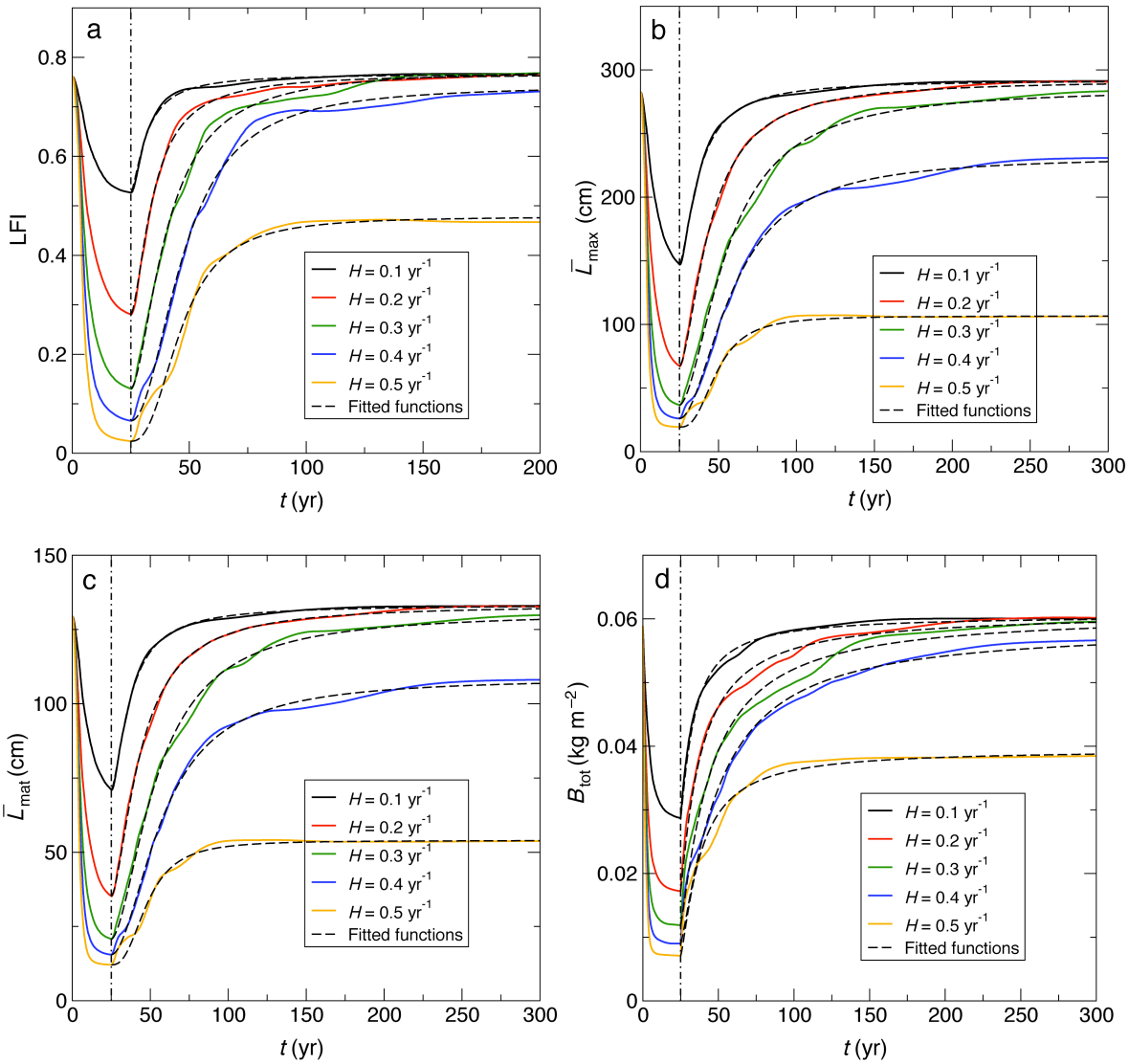

Fig S5. Recovery trajectories across different harvesting rates H for (a) LFI, (b) $\bar{L}_{max}$, (c) $\bar{L}_{mat}$ and (d) B_{tot}, after non-selective fishing for 25 yr. For each trajectory, a power-law function is fitted according to Eq. (1) in the main text. The semi-dashed vertical lines represent the time when fishing stops

LITERATURE CITED

Andersen KH, Pedersen M (2010) Damped trophic cascades driven by fishing in model marine ecosystems. Proc R Soc B 277:795–802

Arditi R, Michalski J (1995) Nonlinear food web models and their responses to increased basal productivity. In: Polis GA, Winemiller KO (eds) Food webs: integration of patterns and dynamics. Chapman & Hall, London

Barnes C, Irigoien X, de Oliveira JAA, Maxwell D, Jennings S (2011) Predicting marine phytoplankton community size structure from empirical relationships with remotely sensed variables. J Plankton Res 33:13–24

Beardall J, Allen D, Bragg J, Finkel ZV and others (2009) Allometry and stoichiometry of unicellular, colonial and multicellular phytoplankton. New Phytol 181:295–309

Berryman AA, Michalski J, Gutierrez AP, Arditi R (1995) Logistic theory of food web dynamics. Ecology 76:336–343

Bersier LF, Kehrli P (2008) The signature of phylogenetic constraints on food-web structure. Ecol Complex 5:132–139

Brown JH, Gillooly JF, Allen AP, Savage VM, West GB (2004) Toward a metabolic theory of ecology. Ecology 85:1771–1789

Cattin MF, Bersier LF, Banašek-Richter C, Baltensperger R, Gabriel JP (2004) Phylogenetic constraints and adaptation explain food-web structure. Nature 427: 835–839

Fauchald P (2010) Predator-prey reversal: a possible mechanism for ecosystem hysteresis in the North Sea? Ecology 91:2191–2197

Fenchel T, Finlay BJ (1983) Respiration rates in heterotrophic, free-living protozoa. Microb Ecol 9:99–122

Folkvord A (2005) Comparison of size-at-age of larval Atlantic cod (*Gadus morhua*) from different populations based on size- and temperature-dependent growth models. Can J Fish Aquat Sci 62:1037–1052

Froese R, Binohlan C (2000) Empirical relationships to estimate asymptotic length, length at first maturity and length at maximum yield per recruit in fishes, with a simple method to evaluate length frequency data. J Fish Biol 56:758–773

Froese R, Pauly D (2010) FishBase (09/2010). www.fishbase.org

Hendriks AJ (1999) Allometric scaling of rate, age and density parameters in ecological models. Oikos 86:293–310

Hendriks AJ (2007) The power of size: a meta-analysis reveals consistency of allometric regressions. Ecol Model 205:196–208

Holling CS (1959) Some characteristics of simple types of predation and parasitism. Can Entomol 91:385–398

ICES (1977) ICES statistical rectangle coding system. ICES Document CM 1977/Gen:3

Jennings S, Pinnegar JK, Polunin NVC, Warr KJ (2002) Linking size-based and trophic analyses of benthic community structure. Mar Ecol Prog Ser 226:77–85

Mackinson S, Daskalov G (2008) An ecosystem model of the North Sea to support an ecosystem approach to fisheries management: description and parameterisation. Science series: technical report No 142. CEFAS

May RM (1976) Estimating *r*: a pedagogical note. Am Nat 110:496–499

Metz JAJ (2008) Fitness. In: Jørgenson SE, Fath BD (eds) Evolutionary ecology, Vol 2 of encyclopaedia of ecology. Elsevier, Oxford

Naisbit RE, Rohr RP, Rossberg AG, Kehrli P, Bersier LF (2012) Phylogeny versus body size as determinants of food web structure. Proc R Soc B 279:3291–3297

Niklas KJ, Enquist BJ (2001) Invariant scaling relationships for interspecific plant biomass production rates and body size. Proc Natl Acad Sci USA 98:2922–2927

Peters RH (1983) The ecological implications of body size. Cambridge University Press, Cambridge

Rossberg AG (2012) A complete analytic theory for structure and dynamics of populations and communities spanning wide ranges in body size. Adv Ecol Res 46:429–522

Rossberg AG, Ishii R, Amemiya T, Itoh K (2008) The top-down mechanism for body-mass– abundance scaling. Ecology 89:567–580

Savage VM, Gillooly JF, Brown JH, West GB, Charnov EL (2004) Effects of body size and temperature on population growth. Am Nat 163:429–441

Sea Around Us Project (2010) http://www.seaaroundus.org/lme

Shephard S, Fung T, Houle JE, Farnsworth KD and others (2012) Size-selective fishing drives species composition in the Celtic Sea. ICES J Mar Sci 69:223–234

van Leeuwen E, Brännström Å, Jansen VAA, Dieckmann U, Rossberg AG (2013) A generalized functional response for predators that switch between multiple prey species. J Theor Biol 328:89–98

van Leeuwen E, Jansen VAA, Bright PW (2007) How population dynamics shape the functional response in a one-predator-two-prey system. Ecology 88:1571–1581

Vincenty T (1975) Direct and inverse solutions of geodesics on the ellipsoid with application of nested equations. Surv Rev 23:88–93

Walters C, Kitchell JF (2001) Cultivation/depensation effects on juvenile survival and recruitment: implications for the theory of fishing. Can J Fish Aquat Sci 58:39–50